1	The FARM (Flexible Array of Radars and Mesonets)	CULTURE - ENCL
2		BON . HITA
3	Joshua Wurman, Karen Kosiba, Brian Pereira, Paul Robinson,	
4	Andrew Frambach, Alycia Gilliland, Trevor White, Josh Aikins	
5	Robert J. Trapp, Stephen Nesbitt	
6	University of Illinois, Champaign, Illinois	
7		
8	Maiana N. Hanshaw	
9	CoreLogic, Boulder, Colorado	
10		
11	Jon Lutz	
12	Unaffiliated, Boulder, Colorado	
13		
14	Corresponding Author: Joshua Wurman, jwurman@illinois.edu	
15		
16	Revision submitted to the Bulletin of the American Meteorological Soci	ety
17	05 March 2021	

1

Early Online Release: This preliminary version has been accepted for publication in *Bulletin of the American Meteorological Society*, may be fully cited, and has been assigned DOI 10.1175/BAMS-D-20-0285.1. The final typeset copyedited article will replace the EOR at the above DOI when it is published.

18 ABSTRACT

- 19 The Flexible Array of Radars and Mesonets (FARM) Facility is an extensive
- 20 mobile/quickly-deployable (MQD) multiple-Doppler radar and in-situ instrumentation
- 21 network.
- 22 The FARM includes four radars: two 3-cm dual-polarization, dual-frequency (DPDF),
- Doppler On Wheels DOW6/DOW7, the Rapid-Scan DOW (RSDOW), and a guickly-
- deployable (QD) DPDF 5-cm COW C-band On Wheels (COW).
- The FARM includes 3 mobile mesonet (MM) vehicles with 3.5-m masts, an array of
- rugged QD weather stations (PODNET), QD weather stations deployed on
- infrastructure such as light/power poles (POLENET), four disdrometers, six MQD upper
- 28 air sounding systems and a Mobile Operations and Repair Center (MORC).
- 29 The FARM serves a wide variety of research/educational uses. Components have
- deployed to >30 projects during 1995-2020 in the USA, Europe, and South America,
- obtaining pioneering observations of a myriad of small spatial and temporal scale
- 32 phenomena including tornadoes, hurricanes, lake-effect snow storms, aircraft-affecting
- turbulence, convection initiation, microbursts, intense precipitation, boundary-layer
- 34 structures and evolution, airborne hazardous substances, coastal storms, wildfires and
- wildfire suppression efforts, weather modification effects, and mountain/alpine winds
- and precipitation. The radars and other FARM systems support innovative educational
- efforts, deploying >40 times to universities/colleges, providing hands-on access to
- 38 cutting-edge instrumentation for their students.

- The FARM provides integrated multiple radar, mesonet, sounding, and related
- 40 capabilities enabling diverse and robust coordinated sampling of three-dimensional
- vector winds, precipitation, and thermodynamics increasingly central to a wide range of
- 42 mesoscale research.
- Planned innovations include S-band On Wheels NETwork (SOWNET) and Bistatic
- 44 Adaptable Radar Network (BARN), offering more qualitative improvements to the field
- project observational paradigm, providing broad, flexible, and inexpensive 10-cm radar
- coverage and vector windfield measurements.

- 47 CAPSULE
- The Flexible Array of Radars and Mesonets (FARM) is a diverse, integrated, robust
- array of mobile / quickly-deployable radars (DOWs/COW), and in-situ, observing
- 50 systems (MM, PODNET, POLENET, Soundings, Disdrometers) used widely for
- research and education.

1. Why FARM?

This paper describes the Flexible Array of Mesonets and Radars (FARM) facility. The FARM is an extensive array of mobile and quickly deployable (MQD) radars, mobile mesonets, quickly deployable (QD) weather stations, sounding systems and disdrometers providing a single source of diverse observational capabilities for research and education. The history, key achievements, capabilities, and future plans for FARM are described.

a. Why mobile/quickly-deployable targeted radar arrays?

Value of radar observations: Narrow-beam, quickly-scanning, meteorological radars have revolutionized the ability of scientists and forecasters to observe the atmosphere. Research and operational radars measure three-dimensional (3D) distributions of radial velocity and precipitation, typically updating every few minutes. A cursory review of the scientific literature reveals the seminal role of radars in research and operational meteorology dating back decades (e.g., Marshall and Palmer 1948; Stout and Huff 1953; Fujita 1965; Houze and Smull 1990; Atlas 1990; Kumjian and Ryzhkov 2008). Many articles using data from radars appear in the refereed literature every month in any of several primary meteorological journals, focusing on scientific advances, forecasting, modeling, and technology. Specialized American Meteorological Society and European radar meteorology conferences focus primarily on radars and their applications. Many colleges and universities offer courses, and there are at least several textbooks (Doviak and Zrnic 1984; Rinehart 1990; Bringi and Chandrasekar

- 2001; Fabry 2015; Rauber and Nesbitt 2018) dedicated to, or with substantial focus
 on, radar meteorology. Radars are one of the core technologies used to guide
 hazardous weather warnings.
- 78 Limitations of stationary radars:
- 79 **Near-ground visibility:** Some phenomena exhibit significant variations near the 80 ground, below typical radar observing horizons. These include tornadoes (e.g., Bluestein and Golden 1993; Wurman et al. 1996; Wurman et al. 2007c; Kosiba and 81 82 Wurman 2013), microbursts (e.g., Fujita 1981; Wilson et al. 1984), snow bands (e.g., Niziol et al. 1995; Steiger et al. 2013), boundary layer fine lines (Wilson and 83 Schreiber 1986; Marquis et al. 2007), hurricane boundary layer rolls (Wurman and 84 Winslow 1998), and wind farm effects (Toth et al. 2011). These near-ground 85 variations are invisible to operational radars such as the Next-Generation Radar 86 (NEXRAD) network of Weather Surveillance Radar-1988 Doppler (WSR-87 88 88D;OFCM 2017), with only ~1% of the NEXRAD observational domain observed below 200 m above radar level (ARL). 89
- **Spatial scales:** Many of these same high-impact phenomena exhibit spatial scales that are too small to observe regularly, or adequately resolve, given the spacing of typical operational radar networks.
- **Temporal Scales:** Finally, many of these same phenomena evolve over very short time scales (Wurman et al. 2007a; Wurman et al. 2013a; Wurman et al. 2014), much shorter than the 120-300 s volumetric update rate of WSR-88Ds, and faster than even the quicker update rates of most research radars (Wurman and Randall 2001).

Spatial and temporal limitations of radar observations are illustrated in Fig 1 where selected phenomena are characterized with very approximate spatial and temporal scales (defined here as the diameter and duration of the phenomena). For example mesocyclones are very approximately 3-10 km in diameter and persist for 1000-3000 s. It takes at least 5 observations across the diameter (or duration) of a phenomenon, each with a beam width (or sample time) \(\frac{1}{4} \) of this distance (or time), to well-resolve its characteristics (measure about 90% of the magnitude) (Carbone et al. 1985). The 1/4scale observations necessary for a mesocyclone to be well-resolved range from 0.8 to 2.5 km, and from about 300 to 800 s. A WSR-88D observing severe weather conducts a volumetric update every 300 s, temporally well-resolving most mesocyclones. However, the ability of WSR-88Ds to well-resolve mesocyclones spatially depends on the range to the mesocyclones, and the resulting beam width of the observations. Very approximately, WSR-88Ds are spaced at 200 km intervals and have 200 km observational domains, so about 50% of mesocyclones occur within 141 km of WSR-88Ds. But, the beam width at 141 km is about 2.5 km, which is barely able to wellresolve detailed characteristics of large mesocyclones. So, while WSR-88D radars can detect mesocyclones through much of their observational doman, they can only well-resolve large mesocyclones over about ½ of that area. Tornadoes, with diameters ranging typically from 100-800 m (Wurman et al 2021) and lifetimes ranging typically from 100-1200 s, require observational scales of 25-200 m and 25-300 s to be wellresolved. This is only achieved when long-lived large tornadoes pass within 4 km of a WSR-88D, i.e., only very rarely. It is important to note that resolving the detailed characteristics of phenomena such as tornadoes, microbursts, and mesocyclones is

98

99

100

101

102

103

104

105

106

107

108

109

110

111

112

113

114

115

116

117

118

119

critical for scientific studies, it is not necessary in order to inform severe weather warnings. WSR-88D data provide great benefit to the warning process through direct detection and indirect inference of the presence or likelihood of these phenomena.

Sparse rapid-scanning phased array networks could well-resolve temporal, but not spatial scales of tornadoes. Dense quick-scanning arrays such as Collaborative Adaptive Sensing of the Atmosphere (CASA: Junyent et al. 2010) can very well-resolve mesocyclones and tornadoes temporally, but cannot spatially well-resolve most tornadoes.

Solution: Adaptable arrays of mobile/quickly-deployable, radars.

The most effective solution to two of these limitations, spatial resolution and lower observing-horizon, is also the simplest: **get closer**.

The most efficacious, moderate-cost, and widely employed solution, pioneered by the Doppler On Wheels (DOW) network, has been the deployment of single or multiple truck-mounted mobile/quickly-deployable (MQD) pencil-beam scanning radars (Wurman et al. 1997). DOWs, and other MQD radars (Bluestein and Pazmany 2000; Biggerstaff et al. 2005; Weiss et al. 2009; Pazmany et al. 2013; NSSL 2021; UAH 2021) have proven particularly valuable tools to observe rare, intermittent, localized, quickly evolving and propagating phenomena, particularly in the common situation where the details of mesoscale phenomena evolution are not well forecast hours in advance. MQD radars target mesoscale phenomena when and where they occur,

increasing the number of sampled phenomena and the quality of observations. MQD DOWs, described below, simply by getting closer and scanning more quickly, are able to resolve the spatiotemporal scales of many important mesoscale phenomena including microbursts, boundary layer thermals, hurricane boundary layer rolls, tornadoes, gust front structures, and lake-effect snow bands. The ability of DOWs to well-resolve the spatial and temporal scales depends on the range to the phenomenon and the duration and evolutionary time-scale of the phenomenon. Referring to Figure 1, DOWs, at typical deployment range of 2-10 km, conducting quick volumetric scans at 20-80 s intervals, are able to well-resolve the spatial and temporal scales of many, but not the smallest tornadoes. Resolving rapid changes in tornado structure, or subtornado scale multiple vortices requires both very fine spatial-scale observations and rapid-scanning, as provided by the Rapid-Scan DOW (RSDOW)(Section 2c).

The DOWs have been deployed semi-permanently (e.g., for weeks or months) in remote locations, anywhere there is even a 4-wheel drive road. These missions include long-term deployments to remote/challenging areas [e.g., ASCII (Geerts et al. 2013), SNOWIE (Tessendorf et al. 2019), OLYMPEX (Houze et al 2017), BRISTOL-HEAD]. Nomadic, chasing, or semi-nomadic missions include VORTEX (Rasmussen et al. 1994), VORTEX2 (Wurman et al. 2012), ROTATE (Wurman 2003; Wurman 2008), TWIRL (Kosiba and Wurman 2016), hurricanes (Wurman and Winslow 1998; Kosiba et al. 2013; Kosiba and Wurman 2014; Wurman and Kosiba 2018), RELAMPAGO (Nesbitt et al. 2021), LLAP (Steiger et al. 2013), OWLeS (Kristovich et al. 2017), PECAN (Geerts et al. 2017), MAP (Bousquet and. Smull 2003), JAWs-Juneau

(Mueller et al. 2004), IPEX (Schultz et al. 2002), and COPS (Wulfmeyer et al. 2011). (See Supplemental Materials Table for listing of research projects and project acronyms)

169

170

171

172

173

174

175

176

177

178

179

180

181

182

183

184

185

186

b.

166

167

168

Why mobile/quickly-deployable targeted surface and sounding arrays? Value and limitations of stationary ground-based observational arrays: In-situ measurements of state variables (e.g., T, RH, P, winds) are critical for understanding meteorological phenomena. However, operational surface and upper-air sounding meteorological networks, including specialized regional surface networks such as the Oklahoma Mesonet (Brock et al. 1995) the West Texas Mesonet (Schroeder et al. 2005), and MESOWEST (Horel et al. 2002), are usually too coarsely distributed to resolve the small scales associated with high-impact atmospheric phenomena. Just as with radars, to well resolve spatial scales < 10 km, in-situ observational spacing << 10 km is required. Tiling a 300 km x 300 km study region at 1 km (or 5 km) spacing, only capable of well-resolving phenomena with scales > 4 km (or > 20 km) (See section 1a) would require 906,000 (301²) (or 3,700 [61²]) instruments, likely an impractical endeavor (see also Trapp 2013, Section 3.5). Even this ambitious stationary design would still be at substantial risk of missing desired events falling outside the study region. Slowly deployable research mesonets (e.g., Foote and Fankhauser 1973; Brock and Govind 1977) have had to choose between very small observational domains and very coarse spacing.

187

188

Solution: Arrays of "mobile", quickly-deployable, ground-based instrumentation.

189 The modern paradigm for obtaining critical in-situ state variable observations in mesoscale studies utilizes adaptable observing systems, which can be easily and 190 quickly deployed ahead of, or during, phenomena of interest. Broadly, these systems 191 fall into three categories: 192 193 194 1. MQD mobile mesonets (MM), where instruments are mounted on vehicles that are driven to phenomena of interest and sample by driving through or near these 195 phenomena (e.g., Straka et al. 1996), 196 197 2. QD instruments that are placed ahead of phenomena and remain stationary 198 199 throughout the data collection [e.g., TOTO (Bedard and Ramzy 1983; Bluestein 1983), Turtles (Brock et al. 1987; Winn et al. 1999), StickNet (Schroeder and Weiss 2008), 200 Florida Coastal Monitoring Program 10-m towers (Master et al. 2010), deployable 201 weather stations (HITPR) (Lee et al. 2004; Wurman and Samaras 2004) disdrometers 202 (Friedrich et al. 2013), and Pods (Wurman et al. 2012)], and, 203 204 3. QD and MQD upper air and boundary layer balloon-borne sounding systems (e.g. 205 Rust et al. 1990; Trapp et al. 2016; Markowski et al. 2018). 206 207 208 Mobile Mesonet transects, QD surface instrumentation, and MQD soundings through

features such as drylines, fronts, storm-generated boundaries and cold pools yield

cross-frontal/boundary data, which allow for mapping and characterizing moisture,

209

wind, and temperature variations that can influence storm initiation, development, and evolution. Targeted in-situ observations using the FARM systems described below, often augmenting DOW or other MQD radar observations, have been, or can be used to increase understanding of a myriad of phenomena including snowbands (Kosiba et al. 2020), urban impacts, wind farm effects, storm anvil and fire plume shadow effects, terrain effects, deep convection (Trapp et al. 2020; Schumacher et al. 2021; Nesbitt et al. 2021), cold pools (Kosiba et al. 2018), hurricanes (Kosiba and Wurman 2009; Kosiba et al. 2013; Wurman et al. 2013c; Wurman and Kosiba 2018; Kosiba and Wurman 2018), and tornadic storms (Markowski et al. 2002; Wurman et al. 2007a; Markowski et al. 2012; Kosiba et al. 2013b; Kosiba and Wurman 2013; Wurman et al. 2013a). (See Supplemental Materials Table).

2. Invention, Development, Deployments of the DOWs and other systems

a. Targeted Single-DOW Observations: DOW1 and successors

While QD, even truck-mounted, non-meteorological radars had existed for decades (Electronics, 1945), and continuous wave (e.g., Bluestein and Unruh 1989) and special purpose mm-wave (e.g., Bluestein et al. 1995) systems had been used in limited applications for research, the DOW radars (Wurman et al. 1997) were the first general-purpose MQD weather radars capable of quick-scanning volumetric data collection, very fine-scale resolution with pulsed transmissions and narrow "pencil-beams", and abilities to penetrate a wide variety of meteorological phenomena using cm-wavelength transmissions.

The first DOW prototype was constructed during October 1994 - May 1995, for < \$50,000, using surplused parts from the National Center for Atmospheric Research (e.g., the old CP-2 radar transmitter, Keeler et al. 1989), a repurposed Econoline Van provided by the National Severe Storms Laboratory, and a surplus SCR-584 antenna (Electronics, 1945). Signal processing and antenna control were hosted on now considered primitive 486 and 286 computers, with data stored on Exabyte tapes. The DOW (later named DOW1) (Fig. 2) deployed during the final weeks of the VORTEX tornado study. New DOW data immediately heralded a qualitative improvement in the ability to observe the fine-scale structure and evolution of tornadoes (e.g., Wurman et al. 1996; Wurman and Gill 2000; Wurman and Kosiba 2013) and a paradigm change for many mesoscale observational studies. The DOW prototype was in a nearly continuous state of evolution as the frontiers of this new technology and its applications were expanded. From 1995-1997, the 1.83 m diameter antenna was replaced with a 2.44 m unit, reducing beamwidth from 1.22° to 0.93°. New, faster and more powerful antenna motors permitted high speed scanning > 50° s⁻¹, even in strong winds, and while driving. A more powerful transmitter and improved signal processing systems and computers were installed. Data were recorded to compact disks (2020-era DOWs would fill one of these compact disks every ~10 s). Faster leveling systems allowed precisely navigated data to be collected < 50 s after parking. Basic specifications of DOW1 and other FARM radars are found in Table 1. The FARM website http://dowfacility.atmos.illinois.edu has links to loops, project descriptions, additional imagery and documentation, data servers, and articles/books describing facility components.

234

235

236

237

238

239

240

241

242

243

244

245

246

247

248

249

250

251

252

253

254

255

258

259

260

261

262

263

264

265

266

267

268

269

270

271

272

273

274

275

276

277

278

279

The new observing paradigm of deploying a high-capability radar near tornadoes enabled the harvesting of many and varied scientific "low hanging fruit" by DOW1 and its successor DOWs (described below). These include the first tornado wind maps, measurements of an axial downdraft and lofted debris (Wurman et al. 1996, Wurman and Gill 2000), multiple vortices (Wurman 2002; Alexander and Wurman 2005), winds versus damage and surface measurement intercomparisons (Wurman and Samaras 2004; Wurman and Alexander 2005, Kosiba and Wurman 2013, Wurman et al. 2013a)(Fig. 4e), winds as low as 3 - 4 m AGL and low-level inflow (Wurman et al. 2007c; Kosiba and Wurman 2013), 3D Ground-Based Velocity Track Display (GBVTD) vector windfield retrievals (Lee and Wurman 2005; Kosiba and Wurman 2010), rapid evolution of debris over varying land use and terrain (Burgess et al. 2002; Kosiba et al. 2012), documentation of cyclonic / anticyclonic tornado pairs and documentation of varied and complex tornado windfield structures including multiple windfield maxima and multiple vortex mesocylones (Wurman and Kosiba 2013), downward propagation of vorticity (Wurman and Alexander 2005) and an extensive climatology of tornado intensity and size revealing, quantitatively, that tornadoes are much more intense and larger than indicated by damage surveys (Wurman et al. 2021). The DOWs have documented the largest and most intense tornado windfields ever measured (Wurman 2003; Wurman et al. 2007c; Wurman et al. 2014), and even, unintentionally, collected data from inside some tornadoes. DOW data were first used to constrain and compare to large eddy simulations of tornado vortices (Kosiba 2009) and laboratory models (Refan et al. 2014), and provide a comparison of tornadic intensity to WSR-

280 88D observations (Toth et al. 2013). DOW data have been integrated with photogrammetric analyses of tornadoes (Wakimoto et al. 2011; Wakimoto et al. 2012). 281 (Multiple-DOW deployments and vector-wind studies are discussed in the next 282 section.) 283 284 The DOW1 was deployed into Hurricane Fran (1996), pionering land-based scientific 285 hurricane intercepts and discovering an unexpected phenomenon, quasi-linear 286 hurricane boundary layer rolls (HBLR) (Wurman and Winslow 1998), found to be 287 288 ubiquitous (e.g., Morrison et al. 2005; Lorsolo et al. 2008; Kosiba et al. 2013) (Fig. 4b). A DOW mission in Hurricane Harvey (2017) revealed the existence of intense Tornado 289 Scale Vortices (TSV) linked to swaths of wind damage and mapped eyewall 290 mesovortices (Wurman and Kosiba 2018) (Fig. 4c). TSVs also were observed in 291 Hurricane Irma (2017) (Kosiba and Wurman 2018). The DOWs documented that tall 292 buildings could cause narrow regions of reduced hurricane winds several km 293 downstream (Wurman et al. 2013b). 294 295 296 It was realized very quickly that DOWs could be utilized in a wide variety of observational programs beyond tornadoes and hurricanes. Immediately after 297 VORTEX, DOW1 was deployed to observe convective initiation and boundary layer 298 299 rolls in SCMS and FLATLAND/LIFT (Weckwerth et al. 1999) and for an MIT microburst study in New Mexico in 1996. Between 1995-2020, DOW1 and its successors were 300 301 deployed to study many different phenomena throughout the United States, including

Alaska and Hawaii, to Canada, Europe, and South America (Fig. 3 and Supplemental

Material Table). Selected scientific highlights include the following: DOWs were first to provide radar evidence of precipitation directly caused by cloud seeding (Tessendorf et al. 2019)(Fig. 4h), the first to map snow band misovortices (Steiger et al. 2013) (Fig. 4d), and first to produce fine-scale radar mapping of fire plumes and hot spots (Wurman and Weygandt 2003). The DOWs mapped fire retardant plumes, simulated aircraft-released toxin plumes, mapped dust devil winds (Wurman et al. 1997), examined coastal low-level jets and their impact on heavy rainfall (Ralph et al. 1999), mapped the flow in alpine valleys (Bousquet and Smull 2003), examined descending reflectivity cores (DRC) in supercells (Byko et al. 2009), documented low reflectivity regions (LRR) in supercells (Wurman et al. 2012; Kosiba et al. 2013b), and mapped boundary layer stratification in Nor'easters (NSF 2015) (Fig. 4g). DOWs have been used extensively to support education (Section 4).

b. Targeted Multiple-DOW Network

The atmospheric equations of motion describe the evolution of 3D vector windfields, not radar-measured Doppler "velocities". Updrafts, downdrafts, rotation, development of clouds and precipitation and lightning are all driven at least in part by 3D vector winds. *It is a rare consumer of Doppler velocity data who would not prefer access to vector windfield measurements.* Techniques for obtaining vector windfields from multiple radar measurements are well established (e.g., Armijo 1969; Ray et al. 1975; Gao et al. 1999; Shapiro et al. 2009), as are more restricted

techniques for inferring 3D winds from single-radar data (e.g., Browning and Wexler 1968; Lee et al. 1994).

In order to obtain fine-scale multiple-Doppler vector wind measurements, all of the individual radars must be close to the targeted phenomena (See Figure 1 in Wurman et al. 1997), which is difficult to achieve with stationary radar networks. This, and the simple benefit of increasing single-DOW observational coverage, motivated the creation of the multiple-DOW network, with the construction of DOW2, in 1997, and its successors.

As was the case with single-DOW deployments, many targeted multiple-DOW deployments harvested "low-hanging scientific fruit". Multiple-DOW tornado "chasing" missions allowed creation of the first fine-scale vector windfield maps of tornadic storms, revealing secondary rear flank gust fronts, fields of vorticity, divergence, tilting of vorticity near tornadoes, and triggers for tornadogenesis (e.g., Wurman et al. 2007ab, Marquis et al. 2008; Wurman et al. 2010; Marquis et al. 2012; Markowski et al. 2012ab; Kosiba et al. 2013b; Markowski et al. 2018), and the first dual-Doppler vector winds resolving tornado structure (with RaXPoL) (Wurman et al. 2016).

Quick, as well as semi-permanent deployments were used to create vector wind mapping of a wide range of other phenomena including non-tornadic supercells (e.g., Beck et al. 2006; Frame et al. 2009), convection initiation and the role of misocyclones (Arnott et al. 2006; Marquis et al. 2007; Zeigler et al. 2007; Friedrich 2008), lake-effect

snow bands and embedded misocyclones (Mulholland et al. 2017; Kosiba et al. 2020), nocturnal mesoscale convective systems (Kosiba et al. 2018; Miller et al. 2020), deep convective storms in complex terrain (Weckwerth et al. 2014; Trapp et al. 2020), and agricultural effects on the boundary layer (Rappin et al. 2021). Fluxes and turbulent kinetic energy (TKE) associated with sub-kilometer scale hurricane boundary layer rolls were quantified (Kosiba and Wurman 2014). The first vector wind retrievals of the boundary layer in a total solar eclipse (Wurman and Kosiba 2018) and in and near wildfire plumes were obtained by DOWs in 2017 and 2020, respectively. Multiple DOWs were used for marine boundary layer studies during CMRP, and for educational missions during PAMREX (Richardson et al. 2008). DOW vector windfields have been integrated with photogrammetric analysis (Atkins et al. 2012) (See Supplemental Materials table).

c. Rapid-Scan DOW

- DOW sampling volumes can be 20,000 times smaller than that typical of WSR-88Ds.
- For example, at typical ranges between targets and these radars:

- WSR-88D resolution volume at 100 km range: $1667 \text{ m x } 1667 \text{ m x } 250 \text{ m} = 7 \text{ x } 10^8 \text{ m}^3$
- DOW resolution volume at 2 km range: 33m x 33m x 25 m = 3 x 10⁴ m³

However, typical DOW *temporal* resolution is only several times better than that of WSR-88D's, 300 s volumes versus 60 s. The DOW-obtained ultra-sharp "snapshots"

of tornadoes revealed that substantial evolution sometimes occurred between observations (Wurman et al. 2007a), limiting the understanding of these evolutionary processes. This effect is clear in Fig. 1, showing how proximate DOWs can well-resolve the spatial scales of tornadoes, but not rapid changes. The need for more rapidly scanning radars has long been known (e.g. Keeler and Frush, 1983). But, rapid-scanning alone, e.g., a network of phased array systems spaced similarly to the current WSR-88D network, results in more frequent but very blurry data (Fig. 1), unable to resolve small spatial-scales. *Balanced fine spatial- and temporal-scale observations are required to fully resolve small and rapidly evolving systems such as tornadoes, microbursts, misocyclones, hurricane boundary layer rolls, boundary layer thermals, rapid fire plume evolution, and the like, motivating the development of the Rapid-Scan DOW (RSDOW) (Wurman and Randall 2001), which became operational in 2003 (Fig. 5).*

The RSDOW employs a relatively inexpensive and "low tech" slotted waveguide antenna. Multiple frequencies are transmitted quasi-simultaneously from a Traveling Wave Tube (TWT) transmitter, in a "frequency-stepped chirp" pulse (see Wurman and Randal 2001), emitting several wavelengths quasi-simultaneously. Unlike slotted waveguide array antennas used in other multi-frequency radars such as ELDORA (Hildebrand et al. 1996), the RSDOW antenna is purposely very dispersive, steering these emissions at different frequencies in different directions, resulting in multiple quasi-simultaneous beams pointing at different elevations (See Fig. 5). The sky is "raked" at several different elevation angles nearly simultaneously. Data from each

frequency, and therefore each differently-pointing beam, are processed separately, as if it were from a different radar, resulting in volumetric data as fast as the antenna completes 360-degree rotations, typically every 7-s. As with all FARM radars, RSDOW archives all raw time series ("IQ", the in-phase and quadrature components of the complex raw signal, see Doviak and Zrnic 1984) data, permitting custom and experimental post-processing, re-sampling, and filtering. Frequency dithering (changing frequency by a few tens of megahertz every ½° of azimuthal scanning, to change beam elevation pointing by about ½°) to improve vertical resolution, and other specialized transmit/receive techniques are possible with the RSDOW, but have not been used to date.

The RSDOW data revealed short-period wind speed oscillations in a tornado (Wurman et al. 2013a) attributed to small spatially-unresolved multiple vortices and documented for the first time that the most intense winds in a different tornado were below 10 m AGL (Kosiba and Wurman 2013). The RSDOW collected fine-temporal resolution data in snowbands during OWLeS, in a variety of supercellular thunderstorms during VORTEX2, measured the rapid evolution of hurricane boundary layer rolls during hurricanes Isabel (2003) (Wurman 2004) and Isaac (2012) (Wurman et al. 2013) and deployed for the CU-TOM and TAMU-SOAP educational projects (See Supplemental Materials table).

The RSDOW platform can be converted to host a traditional radar, for projects which do not require extremely rapid volumetric updates. A 250 kW transmitter, 0.9° beam

parabolic antenna, and different receiver and signal processing replace the specialized RSDOW components, and the system is fielded as DOW8. The RSDOW / DOW8 platform hosts a 14-m pneumatic mast on which anemometers and VHF radio antennas are usually mounted. Temperature (T), relative humidity (RH), and pressure (P) instrumentation are mounted to the truck. A scissor lift can raise the pedestal about 2-m so that the antenna is above the height of the operator and driver cabin, but this has not, to date, been used during a mission.

d. Quick-Scanning Dual-Polarization DOWs

Dual-polarization radars (Bringi and Chandrashekar 2001; Fabry 2015; Rauber and Nesbitt 2018; Bringi and Zrnic 2019) have been used in meteorological research dating back to the 1980's (e.g. Wakimoto and Bringi 1988) to provide observations distinguishing hail, drop size, and other precipitation particle characteristics.

Recognizing the added information provided by dual-polarization capabilities, the WSR-88D network was upgraded to dual-polarization from 2011 - 2013. The University of Massachusetts MQD radar was upgraded to dual-polarization, obtaining pioneering observations of tornado debris clouds (Bluestein et al. 2007). The NOAA NOXP became operational prior to deploying in Hurricane Ike in 2008 (NSSL 2021). The University of Alabama upgraded the ARMOR radar in 2004 (Petersen et al. 2005).

obtain the necessary independent samples required for accurate dual-polarization

- 440 measurements (Bringi and Chandrashekar 2001). Slow-scanning is an anathema for targeted short-temporal scale studies of rapidly evolving phenomena (see Fig. 1). So, 441 to permit more balanced temporal and spatial scale dual-polarization observations, two 442 DOWs (DOW6 and DOW7) were upgraded to dual-polarization, employing a unique 443 dual-polarization, dual-frequency design (DPDF). The DPDF technique involves 444 445 transmitting two frequencies quasi-simultaneously, separated by 150 MHz. This permits independent samples from each frequency to be combined, allowing for high 446 quality ZDR calculations while scanning twice as fast. The DPDF DOWs employ a 447 448 unique polarization switching array (Fig. 6) permitting two different transmit/receive modes: 449
- ("Fast-45") both frequencies transmit at 45° polarization orientation (by transmitting equal power at both horizontal and vertical polarizations simultaneously) and
 measure returned horizontal and vertical signals in order to calculate differential reflectivity (ZDR), cross-polarization correlation coefficient (ρHV) and differential phase (ΦDP) in both frequencies, and

455

456

457

458

- ("LDR+45") One frequency is emitted with a horizontal polarization angle, permitting calculation of linear depolarization ratio (LDR) through comparison of horizontal and vertical polarization returns. The 2nd frequency is transmitted at 45° orientation, as described above, allowing calculation of ZDR, pHV and Φ-DP. LDR+45 mode was first used during RELAMPAGO (Trapp et al. 2020).
- The DPDF DOWs archive all raw time series ("IQ") data, permitting custom and experimental post-processing, re-sampling, and filtering. DPDF DOWs were used in VORTEX2, LLAP, TWIRL, GRAINEX, SNOWIE, ASCII, OWLeS, PECAN, and

RELAMPAGO (See Supplemental Materials table). The DPDF DOW platforms host 18-m pneumatic masts on which anemometers and VHF radio antennas are usually mounted. T, RH, P instruments are mounted to the trucks.

466

467

465

463

464

e. C-band On Wheels (COW)

468

469

470

471

472

473

474

475

476

477

478

479

480

481

482

483

484

The FARM (and all other MQD) radars employ antennas smaller than 2.5 m so that the trucks plus antennas can fit on roads and under bridges. In order to focus narrow, <= 1° beams, most MQD radars transmit using 3-mm (W-band) to 3-cm (X-band) wavelengths. The paramount goal of fine-scale resolution is achieved, but at the cost of severe attenuation in heavy precipitation, common in high impact mesoscale systems. A notable exception has been the C-band (~5.5 GHz or 5 cm) SMART Radars (SRs) (Biggerstaff et al. 2005), which suffer less attenuation (Fig. 7) (see, e.g., Doviak and Zrnic 1984). But, this ability comes with a cost. The SR's 2.4 m antennas produce broader beamwidths (1.6°) and > 2.5 times larger resolution volumes (1.6°/0.93° horizontal x 1.6°/0.93° vertical) compared to X-band MQD radars such as the DOWs. The compromises inherent with X- and C-band mobile radars were experienced during VORTEX2 when SR2 and DOW6 simultaneously observed a tornadic supercell from similar ranges. The DOW6 observations were severely attenuated through the core, particularly behind the hook echo. SR2 observations severely under-resolved the tornadic circulation, with observed shear of only 57 m s⁻¹ compared to the DOWs measurement of 84 m s⁻¹, a reduction of 32% (Fig. 7).

In order to avoid the compromises inherent to existing X- and C-band MQD radars, the C-band On Wheels (COW) was developed in 2018, using a unique quickly-assembling antenna design. The COW travels with its antenna in two pieces (Fig 8). Then, using an on-board crane, this antenna is quickly assembled on-site, to its full 3.8 m diameter, resulting in a 1.05° beam. *Low attenuation and fine-scale resolution are achieved simultaneously.* Naturally, there is a compromise: the COW cannot "chase" since it requires ~2 hours for set up and tear down. But, the COW is ideal for most targeted observational projects, including those similar to RELAMPAGO, PECAN, PERILS, IHOP, CALJET, and hurricanes, deploying up to once-per-day. And it can be deployed for longer periods for projects similar to OLYMPEX, GRAINEX, SNOWIE, and ASCII, and can also serve as a "gap filler" radar. Like the DOWs, the COW employs DPDF technology for fast-45 dual-polarization and 45+LDR capability. COW uses dual 1 MW transmitters, by far the most powerful in any QD or MQD radar, for maximum sensitivity.

3. MM, Pods, Poles, Soundings, MORC

To provide a robust, integrated, and flexible in-situ observational network deployable in coordination with the DOW/COW network, and to improve on existing designs for such observational systems, FARM includes an innovative, evolving and diverse array of mobile mesonet (MM) and QD observational ground-based systems (PODNET, POLENET), several mobile upper air sounding systems, a Lagrangian "swarmsonde"

balloon system, and a mobile operations center (MORC). Specifications are found inTable 2.

510

511

512

513

514

- a. **Mobile Mesonet (MM):** Pickup-truck based MM with instruments that collect standard meteorological observations of T, RH, P, and wind incorporating pioneering forward-mounted 3.5 m AGL masts to avoid vehicle slipstream (Fig. 9). MMs carry PODNET units (see deployment of Pods from a MM in Fig. 10), balloon-borne sounding systems, and disdrometers and can tow systems such as 915 MHz profilers.
- b. **PODNET:** A pioneering array of QD ruggedized weather stations (Pods).
 Deployed from MM, Pods collect standard meteorological observations of T, RH, P,
- and wind at 1, 1.5, or 2 m AGL (depending on configuration), and video or time lapse photographs (Fig. 10).
- 520 c. **Disdrometers:** The facility hosts several Parsivel systems, which can be paired 521 with dual-polarization radars and are often deployed with PODNET units.
- d. **POLENET:** Often there is a need to obtain near-surface wind and other 522 meteorological observations where there may be no solid and level ground, road 523 524 shoulder, and/or at altitudes above 2 m AGL (in less open terrain, near fences, guard rails, road signs, or at flood-prone sites, etc., e.g., in a hurricane). The FARM includes 525 an array of QD, fully configurable, rugged instruments comprising POLENET. These 526 527 are attached with clamps and/or straps to existing infrastructure such as telephone and power poles, bridge railings, dock railings, lighting poles, and similar structures (Fig. 528 11), in order to measure wind, T, P, and RH. 529

- e. **Soundings**: Several GRAW and one Windsond/Swarmsonde balloon-borne sounding systems are operated from MMs, DOWs, or other vehicles to provide adaptable/targeted upper air and boundary layer sounding capability (Fig. 12).
 - f. **Mobile Operations and Repair Center (MORC):** Complex highly mobile (chasing) projects such as VORTEX2, ROTATE, and TWIRL, or projects with special needs (e.g. MASCRAD) may require a mobile operations/coordination center, data management office, and repair facility, or a field headquarters vehicle. The Mobile Operations and Repair Center (MORC) is a long sprinter van with multiple scientist/engineer work stations, a wall of monitors, a computer rack, and two generators. A 10-m pneumatic mast houses weather instruments and a high-powered VHF radio for communications with mobile or remote fleets (Fig. 13).

The FARM MMs, with evolving designs, were used to obtain transects in and near supercellular thunderstorms and tornadoes (ROTATE, VORTEX2, TWIRL)(Fig. 4e), and even obtained, accidentally, observations from inside a tornado (Kosiba and Wurman 2013). PODNET was initially designed to obtain multiple transects of low-level tornado winds. The very simple and inexpensive and robust design allowed for many PODNET units to be constructed, and "picket fence" type deployments ahead of tornadoes to be attempted. Pods obtained wind data very near tornadoes (Kosiba et al. 2016; Wurman et al. 2016; Kosiba et al. 2020b), revealing high potential temperature inflow towards tornadoes and possible inflow jets. Efforts continue to achieve the full picket fence style of deployment. PODNET was deployed on sea walls during Hurricane Ike, where it was too hazardous for manned-instruments (Kosiba and

Wurman 2009), and during Hurricanes Gustav, Isaac, Harvey, and Irma (Wurman et al.

2013c; Wurman and Kosiba 2018; Kosiba and Wurman 2018). Prototyping of

POLENET occurred during hurricane Florence (2018) and it deployed to collect ~4 m

AGL winds in the landfall region of hurricane Delta (2020). (Fig. 11).

The MMs and Pods documented thermodynamic variations across lake-effect snowbands during OWLeS (Kosiba et al. 2020), thunderstorm-generated cold pools during PECAN (Kosiba and Wurman)(Fig. 4f) and RELAMPAGO (Trapp et al. 2020; Nesbitt et al. 2021), and in New England Coastal Storms (NSF 2015). The FARM MQD upper air sounding systems have been used in several studies including PECAN, MASCRAD, GRAINEX, and RELAMPAGO and the Swarmsonde system was first used in severe convection in 2020. The facility's disdrometers were used in PECAN and

4. Education and outreach

RELAMPAGO.

The simplicity, transportability, and adaptability of the DOW radars has facilitated their broad use in education and outreach (Fig 14). Often MM, Pods, and/or soundings are used in tandem with a DOW to provide a broader educational experience. *FARM is designed to be a national educational resource.* The DOWs, and other instrumentation, have participated in over 40 education and outreach projects at a variety of colleges and universities nationwide, most without major instrumentation programs themselves. These include small institutions, Historically Black Colleges and Universities (HBCU) and Tribal Colleges and Universities (TCU), resulting in

unusual and especially rich, hands-on exposure to otherwise unavailable state-of-theart instrumentation. The DOWs have been integrated into radar, other meteorology, and environmental science courses (e.g., Richardson et al. 2008, Bell et al. 2015; Milrad and Herbster 2017) and have been used to facilitate local community and K-12 outreach. With only minor training, students can fully operate DOWs, resulting in hands-on, fully participatory educational experiences in experimental design, field data collection, and data analysis. Some student-designed projects have led to formal publications (e.g., Toth et al. 2011). The DOWs and associated instrumentation have been the highlight of small, large, and very large outreach activities both locally and nationwide, including a 20-museum national tour associated with an IMAX movie featuring DOW science missions, national events such as the USA Science and Engineering festival, and multi-school tours such as occurred in Missouri in 2012. FARM instrumentation, data, and/or scientists have been featured in two IMAX films, Forces of Nature and Tornado Alley, several documentaries including National Geographic's The True Face of Hurricanes and Tornado Intercept, Public Broadcasting's NOVA, and the Discovery Channel's Storm Chasers television series, as well as in other media including CBS, NBC, CNN, BBC, NHK, El Globo, TV Asahi, Al Jazeera, VOA, and many others. Articles discussing FARM instrumentation and/or data have appeared in the New York Times, Washington Post, Economist, Der Speigel, Discover, Popular Science, New Scientist, USA Today, Scientific American, and many other high impact publications. Several dozen popular books and textbooks use images or data from FARM instrumentation.

598

576

577

578

579

580

581

582

583

584

585

586

587

588

589

590

591

592

593

594

595

596

5. Data, Calibration, Displays, Field Coordination

Calibration and data quality control are critical for radars, especially for reflectivity and dual-polarization fields. System calibrations are conducted by injecting signals through a range of intensities, and by measuring gains and losses of individual and groups of components. Quasi-periodic vertically pointing scans during precipitation provide calibration for ZDR. (Under most circumstances, ZDR is expected to be zero when measured at zenith. Additionally, the average of ZDR through a 360 degree rotation of a zenith-pointed antenna is expected to be zero even in the presence of strong electrical fields, or wind shear. Deviations from this average are considered error and can be subtracted from raw ZDR fields, see Hubbert et al. 2003) Intercomparisons with other FARM radars, other research radars, and WSR-88D are made, when possible. Calibrations of MM, PODNET, and POLENET instruments are conducted primarily through intercomparisons among the many FARM systems.

Data from the FARM, including full time series IQ data from DOWs/COW, frequently requires tens of terabytes (TB) of storage capacity, sometimes exceeding 100 TB.

Data are stored on relatively inexpensive NAS disk arrays. Physical and cyber data security is achieved through triple redundancy, with one backup copy retained offline and another copy physically remote. Data are typically available through FTP, except for the extremely large time series collections, which are transferable physically.

The FARM facility has developed and maintains a custom suite of radar and instrument data display and field tracking software, the Geographical Unified Radar Utility (GURU)

(Fig. 15). This was prototyped for the RELAMPAGO operations center and provides real-time DOW/COW radar displays as well as MM and PODNET deployments, and sounding flight tracks. Radar editing tools for GURU are in development to facilitate enhanced radar data perusal including dealiasing, deglitching, and other data quality functions.

6. Future FARM instrumentation

The FARM exists to provide cutting-edge, forward-looking instrumentation capabilities for a wide range of meteorological studies and education. Since its inception, the DOW facility, now FARM, has innovated ambitiously, inventing new and broadly useful observational capabilities and techniques (e.g., DOWs themselves, the RSDOW, POLENET, the COW). We envision this inventive mission continuing, including two major innovations to greatly enhance community observational capabilities.

a. S-band On Wheels (SOW) and SOWNET

Long wavelength, 10-cm (S-band) radars with the ability to penetrate deeply through intense precipitation provide critical operational (WSR-88D) and research capabilities (e.g. S-POL, Lutz et al. 1995; CHILL, Brunkow et al. 2000; NPOL, Petersen and Wolff 2013).

Stationary or quasi-stationary/transportable radars have design freedom to use large antennas since they are not constrained by road worthiness. The narrow beams and superior precipitation penetrating ability of 10-cm systems allow observations in a variety of intensely precipitating phenomena. Superior Bragg scattering sensitivity permits clear-air observations out to > 100 km range. Thus, S-band radars have been core instrumentation for many meteorological studies.

However, since they employ cumbersome, heavy, 8 m diameter antennas, they are very expensive, and difficult and slow to assemble and deploy. Usually, only one radar is deployed, obtaining only single-Doppler measurements.

We envision a new concept, an S-band On Wheels Network (SOWNET) (Fig. 16), comprising multiple quickly-deployable, S-band truck-borne radars, to address these limitations. A network of 4 SOWs, SOWNET, will replace a single large S-band 1° beamwidth radar with an array of smaller, 5.5 m (18') antenna, quickly-deployable, 1.5° beamwidth truck-borne radars. Of course, broader beams result in *potentially* coarser data. But, deployed in arrays, one or more SOWs are nearly always reasonably close to targeted phenomena, so *SOWNET resolution over most of a study area is usually better than that of a single large radar.* We plan to develop a prototype SOW system in the anticipation of deploying future SOWNET.

The key advantages of SOWNET are:

- 1,2,3, or 4 SOWs can comprise a SOWNET deployment, customizing for small and large missions.
- Resolution resulting from a few SOWs is better than a single large radar.
- 5.5 m (18') diameter antennas: < ½ sail-area, < ½ weight, compared to 1.0
- degree 8 m (26') diameter antennas, reducing power needs and set up time
- SOWs can be assembled with a crew of 3, in ~6 hours.
- Total time to deploy entire SOWNET array = ~5 days
- 672 SOWNET entire network deployment is $< \frac{1}{2}$ the cost to deploy compared to
- 673 S-POL, based on much reduced staffing needs and total set up time.
- SOWs can be operated by lightly trained student crews
- SOWNET arrays can be polygons or quasi-linear, and can change during a
- 676 project.
- Reliability is enhanced by eliminating single points of failure; if one SOW breaks,
- others in the network still provide multi-radar coverage.
- **SOWNET** is automatically multiple-Doppler.
- Each SOW provides independent dual-polarization observations.
- SOWNET will employ DPDF technology to scan twice as fast as current large
- 682 radars.
- SOWNET will employ dual 1-MW transmitters, resulting in greater sensitivity in
- the clear-air boundary layer compared to existing radars which employ single
- 685 transmitters.

686

687

b. Bistatic Adaptable Radar Network (BARN)

- While DOWs have provided targeted multiple-Doppler vector wind observations for myriad projects, multiple-Doppler deployments remain difficult and expensive.
- 690 Bistatic systems (e.g., Wurman et al. 1993; Wurman 1994; Protat and Zawadzki 1999; Friedrich al. 2000, Satoh and Wurman 2003), particularly mobile units, offer an 691 inexpensive logistically easier capability to observe 3D vector windfields. They comprise 692 a traditional transmitting and scanning radar paired with one to many remotely deployed 693 receivers with non-scanning low to medium gain antennas. Vector winds are calculated 694 695 from simultaneous measurements in the native coordinate system of the transmitting/receiving radars (no spatial or temporal interpolation required). Bistatic 696 receivers use small antennas, have no expensive transmitters, and can be deployed 697 698 similarly to PODNET units or carried on small vehicles like MM.
- We plan to incorporate a network of MQD bistatic receivers, BARN, integrated with
 SOWs, DOWs, and COW, to provide critical vector windfields. This will form the
 backbone for many future research projects requiring dual-polarimetric, near-ground,
 fine-scale, vector wind observations (Fig. 17).
- 703 The key features of BARN are:
- BARN enables multiple-Doppler vector wind measurements over targeted
 regions.
- While SOWNET is providing moderate-resolution multiple-Doppler measurements,
 BARN provides finer-scale and/or customized measurements over smaller
 domains.

- BARN units will be configured to couple with different SOWS, COW, or DOWs.
 Only the receiver front ends and antennas are frequency-specific.
- BARN units will be stationary, deployed for the duration of a project, or mobile.
- Stationary BARN units will be unattended, low power, and logistically similar
 to deployable weather stations.
- Highly redundant BARN units provide extreme reliability of multiple-Doppler
 operations.
- BARN units are < 1/10 the cost of scanning transmitting radars.
- BARN receiving antennas will be designed with different characteristics. These will
 include previously-used low-gain systems optimized to sample broad areas of
 precipitation, but unable to observe clear-air non-precipitating regions., Medium gain systems, perhaps slowly scanning or switching, which can obtain vector wind
 measurement in the non-precipitating boundary layer will be designed. Different
 configurations will be optimized for different observational needs.

723

724

725

726

727

728

729

730

7. Summary

Since 1995 the DOWs and other instrumentation comprising FARM have facilitated a broad and diverse range of observational studies, education, and outreach. DOWs in particular have facilitated a new observational paradigm for many meteorological projects, and are frequently used in conjunction with other FARM systems including PODNET, MMs, disdrometers, and POLENET. The extensive array of FARM instrumentation, comprising 4 MQD radars, a fleet of MM, PodNet, PoleNet,

- 731 Soundings, Disdrometers, the MORC, and future systems, will continue to be the backbone of many major research studies, often complemented by additional 732 instrumentation such as LIDARs, Unmanned Aerial Systems (UAS), other MQD radars, 733 MM, manned research aircraft, and QD weather stations (e.g., UAS in VORTEX2, 734 Riganti and Houston 2017, LIDAR and multiple aircraft in PECAN, Geerts et al. 2016). 735 736 FARM instrumentation has been designed and operated with ease of use, student operability, and low cost in mind. 737 From 2008-2019 these facilities were supported by and available through the Lower 738 Atmospheric Observing Systems (LAOF) program at the National Science Foundation 739 (NSF). This permitted these systems to be used for not only large field projects (e.g., 740 RELAMPAGO, PECAN, VORTEX2), but a variety of smaller single- to several-741 investigator studies (e.g., OWLeS, SNOWIE, MASCRAD, ASCII, GRAINEX, 742 743 OLYMPEX). LAOF also supported frequent educational and extensive outreach deployments, impacting thousands of students, and tens of thousands in the general 744 public. FARM, now managed through the University of Illinois, remains available to 745 researchers and educators by request (See http://dowfacility.atmos.illinois.edu), and it 746 is hoped that methods of support and request, enabling the previously broad and 747 diverse access possible through LAOF, will again be realized. As of the time of writing, 748 projects potentially employing FARM instrumentation to study tornadoes, quasi-linear 749 convective systems, mountain/valley wind systems, convective initiation, New England 750
- We expect an active future for FARMing.

are in various stages of planning.

751

752

winter storms, Northeastern ice and snow storms, hurricanes, and other phenomena

Acknowledgements

754

755

756

757

758

759

760

761

762

763

764

765

766

767

768

769

770

771

772

773

The FARM comprises observational systems developed, constructed, maintained and operated over 26-plus years. We thank the literally hundreds of operators, drivers and other supporters of the dozens of educational and research missions, including Curtis Alexander, Steve Weygandt, David Dowell, Scott Richardson, Yvette Richardson, Herb Stein, Jerry Straka and Erik Rasmussen from the early years. We thank the engineers, software engineers and scientists at the National Center for Atmospheric Research, especially Mitch Randall, Chris Burghart, Eric Loew, Mike Dixon, Jeff Keeler, Jim Wilson, and Dave Carlson, the staff of the Center for Severe Weather Research (CSWR), especially Ling Chan, Justin Walker, Rachel Humphrey, Danny Cheresnick, Jim Marquis, Traeger Meyer, and the many experts in the radar meteorology community who provided wisdom over the years, including Earle Williams, Dave Atlas, Isztar Zawadski, Fredric Fabry, Dusan Zrnic, Dick Doviak, Paul Markowski, and Katja Friedrich. Support for the FARM, its DOW Facility precursor, and its missions was provided by the National Science Foundation, the National Oceanic and Atmospheric Administration, the Department of Energy, the Department of Defense, the United States Forest Service, the Discovery Channel, National Geographic, the National Aeronautical and Space Administration, the University of Oklahoma, the University of Illinois, the State of Colorado, and several other sources.

Data Availability Statement

This paper does not describe any particular data sets. Data from the FARM will be available through the FARM Facility by contacting its managers.

776 **References**

777

- Armijo, L., 1969: A theory for the determination of wind and precipitation velocities with
- 779 Doppler radar. *J. Atmos. Sci.*, **26**, 570–573.

780

- Alexander, C.R., J. Wurman, 2005: The 30 May 1998 Spencer, South Dakota, Storm.
- Part I: The Structural Evolution and Environment of the Tornadoes. *Mon. Wea. Rev.*,
- 783 **133**, 72-97.

784

- Arnott, N.R., Y.P. Richardson, J. Wurman, E.M. Rasmussen, 2006: Relationship
- between a Weakening Cold Front, Misocyclones, and Cloud Development on 10 June
- 787 2002 during IHOP. *Mon. Wea. Rev.*, **134**, 311-33.

788

- Atkins, N. T., A. McGee, R. Ducharme, R.M. Wakimoto, J. Wurman, 2012: The
- 790 LaGrange Tornado during VORTEX2. Part II: Photogrammetric Analysis of the
- Tornado Combined with Dual-Doppler Radar Data. *Mon. Wea. Rev.*, **140**, 2939-2958.

792

- 793 Atlas, D. (ed), 1990: Radar in meteorology: Battan Memorial and 40th Anniversary
- 794 Radar Meteorology Conference. American Meteorological Society, 806 pp.

795

- Beck, J.R., J.L. Schroeder, J. Wurman, 2006: High-Resolution Dual-Doppler Analyses
- of the 29 May 2001 Kress, Texas, Cyclic Supercell. *Mon. Wea. Rev.*, **134**, 3125-3148.

- Bedard, Jr., A. J., and C. Ramzy, 1983: Surface Meteorological Observations in Severe
- Thunderstorms, Part I: Design Details of TOTO. J. Appl. Meteor. Climatol., 22, 911-
- 801 918.
- Bell, M.M., R.A. Ballard, M. Bauman, A.M. Foerster, A. Frambach, K.A. Kosiba, W.-C.
- Lee, S.L. Rees, J. Wurman, 2015: The Hawaiian Educational Radar Opportunity
- 804 (HERO). Bull. Amer. Meteor. Soc., **96**, 2167-2181.

- 806 Biggerstaff, M. I., and Coauthors: The Shared Mobile Atmospheric Research and
- Teaching Radar: A Collaboration to Enhance Research and Teaching. *Bull. Amer.*
- 808 *Meteor. Soc.*, **86**, 1263-1274.

809

- Bluestein, H. B., 1983: Surface Meteorological Observations in Severe Thunderstorms:
- Field Measurements and Design Detail of TOTO, J. Appl. Meteor. Climatol., 22, 919-
- 812 930.
- 813 Bluestein, H. B., and W. P. Unruh, 1989: Observations of the windfield in Tornadoes,
- Funnel Clouds, and Wall Clouds with a Portable Doppler Radar, *Bull. Amer. Meteor.*
- 815 *Soc.*, **70**, 1514-1525.
- 816 Bluestein, H. B., and J. H. Golden, 1993: A review of tornado observations. *The*
- Tornado: Its Structure, Dynamics, Prediction and Hazards, Geophys. Monogr., No. 79,
- 818 Amer. Geophys, Union, 19–39.

- Bluestein, H. B., A. L. Pazmany, J. C. Galloway, and R. E. McIntosh, 1995: Studies of
- the Substructure of Severe Convective Storms Using a Mobile 3-mm-Wavelength
- 822 Doppler Radar, *Bull. Amer. Meteor. Soc.*, **76**, 2155-2170.
- Bluestein, H. B., and A. L. Pazmany, 2000: Observations of tornadoes and other
- convective phenomena with a mobile, 3-mm wavelength, Doppler radar: The spring
- 1999 field experiment. *Bull. Amer. Meteor. Soc.*, **81**, 2939–2951.
- Bousquet, O., B.F. Smull, 2003: Airflow and Precipitation Fields within Deep Alpine
- Valleys Observed by Airborne Doppler Radar. J. Appl. Meteor., 42, 1497-1513.
- 828
- Bringi, V. N., and V. Chandrasekar, 2001: *Polarimetric Doppler Weather Radar:*
- Principles and Applications. Cambridge University Press, 636 pp.
- 831
- Bringi, V., and Z. Dusan, 2019: Polarization Weather Radar Development from 1970–
- 1995: Personal Reflections. *Atmosphere*, **10**, 714.
- 834
- Brock, F. V., and P. K. Govind, 1977: Portable Automated Mesonet in Operation. J.
- 836 Appl. Meteor. Climatol., **16**, 299-310.
- 837
- Brock, F. V., G. Lesins, and R. Walko, 1987: Measurement of Pressure and Air
- 839 Temperature Near Severe Thunderstorms: An Inexpensive and Portable
- 840 Instrument. Extended Abstracts, 6th Symp. on Meteorological Observations and
- Instrumentation, New Orleans LA, Amer. Meteor., 320-323.

- Brock, F. V., K. C. Crawford, R. L. Elliott, G. W. Cuperus, S. J. Stadler, H. L. Johnson
- and M. D. Eilts, 1995: The Oklahoma Mesonet: a technical overview. *J. Atmos.*
- 844 Oceanic Tech., **12**, 5-19.

- Browning, K. A., and R Wexler, 1968: The determination of kinematic properties of a
- windfield using Doppler radar. *J. Appl. Meteor*, **7**, 105–113.

848

- Brunkow, D., V. N. Bringi, P. C. Kennedy, S. A. Rutledge, S. V. Chandrasekar, E. A.
- Mueller, and R. K. Bowie, 2000: A Description of the CSU-CHILL National Radar
- 851 Facility, *J. Atmos. Oceanic Technol.*, **17**, 1596-1608.

852

- Burgess, D. W., M. A. Magsig, J. Wurman, D. C. Dowell, and Y. Richardson, 2002:
- Radar Observations of the 3 May 1999 Oklahoma City Tornado, Wea. Forecasting, 17,
- 855 **456-471**.

856

- Byko, Z., P. Markowski, Y. Richardson, J. Wurman, E. Adlerman, 2009: Descending
- 858 Reflectivity Cores in Supercell Thunderstorms Observed by Mobile Radars and in a
- High-Resolution Numerical Simulation. *Wea. and Forecasting*, **24**, 155-186.

860

- Carbone, R. E., M. J. Carpenter, and C. D. Burghart, 1985: Doppler Radar Sampling
- Limitations in Convective Storms, J. Atmos. Oceanic Technol., 2, 357-361.

864 Doviak, R. J., and D. S. Zrnic, 1984: Doppler radar and weather observations, 1st ed. Academic Press., 470 pp. 865 866 Electronics, Nov 1945, The SCR-584 Radar. 104 p. 867 868 Fabry, F., 2015: Radar Meteorology: Principles and Practice, Cambridge University 869 Press, 276 pp. 870 871 Foote, G. B., and J. C. Fankhauser, 1973: Airflow and Moisture Budget Beneath a 872 Northeast Colorado Hailstorm. J. Appl. Meteor. Climatol., 12, 1330-1353. 873 874 Frame, J., P. Markowski, Y. Richardson, J. Straka, and J. Wurman, 2009: Polarimetric and Dual-Doppler Radar Observations of the Lipscomb County, Texas, Supercell 875 Thunderstorm on 23 May 2002. Mon. Wea. Rev., 137, 544-561. 876 877 Friedrich, K., M. Hagen, and P. Meischner, 2000: Vector windfield determination by 878 879 bistatic multiple-Doppler radar. *Phys. Chem. Earth*, 25B, 205–1208. 880 Friedrich, K., D. E. Kingsmill, C. Flamant, H. V. Murphey, and R. M. Wakimoto, 2008: 881 Kinematic and Moisture Characteristics of a Non-precipitating Cold Front Observed 882

during IHOP. Part II: Alongfront Structures. Mon. Wea. Rev., 136, 3796-3821.

883

- Friedrich, K., E. Kalina, F. Masters, and C. Lopez, 2013: Drop-Size Distributions in
- Thunderstorms Measured by Optical Disdrometers during VORTEX2, Mon. Wea. Rev.,
- 887 **141**, 1182-1203.

- Fujita, T. T., 1965: Formation and steering mechanisms of tornado cyclones and
- associated hook echoes. Mon. Wea. Rev., 93, 67–78.

891

- Fujita, T.T., 1981: Tornadoes and downbursts in the context generalized planetary
- 893 scales. *J. Atmos. Sci.*, **38**, 1511-1534.

894

- Gao, J., M. Xue, A. Shapiro, and K. K. Droegemeier, 1999: A variational method for the
- analysis of three-dimensional windfields from two Doppler radars. *Mon. Wea. Rev.*,
- 897 **127**, 2128–2142.

898

- Geerts, B., B. Pokharel, K. Friedrich, D. Breed, R. Rasmussen, Y. Yang, Q. Miao, S.
- Haimov, B. Boe, and E. Kalina, 2013: The Agl Seeding Cloud Impact Investigation
- 901 (ASCII) campaign 2012: overview and preliminary results. *J. Wea. Mod.*, **45**, 24-43.

- Geerts, B., D. Parsons, C.L. Ziegler, T.M. Weckwerth, D.D. Turner, J. Wurman, K.A.
- Wosiba, R.M. Rauber, G.M. McFarquhar, M.D. Parker, R.S. Schumacher, M.C.
- Coniglio, K. Haghi, M.L. Biggerstaff, P.M. Klein, W.A. Gallus Jr., B.B. Demoz, K.R.
- 806 Knupp, R.A. Ferrare, A.R. Nehrir, R.D. Clark, X. Wang, J.M. Hanesiak, J.O. Pinto, J.A.

- 907 Moore, 2017: The Plains Elevated Convection at Night (PECAN) Field Project, Bull.
- 908 Amer. Meteor. Soc., **98**, 767-786

- Hildebrand, P. H., W.-C. Lee, C. A. Walther, C. Frush, M. Randall, E. Loew, R. Neitzel,
- 911 R. Parsons, J. Testud, F. Baudin, and A. LeCornec, 1996: The ELDORA/ ASTRAIA
- airborne Doppler weather radar: High-resolution observations from TOGA COARE.
- 913 Bull. Amer. Meteor. Soc., **77**, 213-232.

914

- Horel, J., M. Splitt, L. Dunn, J. Pechmann, B. White, C. Ciliberti, S. Lazarus,
- J. Slemmer, D. Zaff, and J. Burks, 2002: MESOWEST: Cooperative Mesonets in the
- 917 Western United States. Bull. Amer. Meteor. Soc., 83, 211-226.
- Houze, R. A., B. F. Smull, B. F., and P. Dodge, 1990: Mesoscale Organization of
- 919 Springtime Rainstorms in Oklahoma, *Mon. Wea. Rev.*, **118**, 613-654.

920

- Houze, R., L. McMurdie, W. Petersen, M. Schwaller, W. Baccus, J. Lundquist, C. Mass,
- B. Nijssen, S. Rutledge, D. Hudak, S. Tanelli, G. Mace, M. Poellot, D. Lettenmaier, J.
- 23 Zagrodnik, A. Rowe, J. DeHart, L. Madaus, and H. Barnes, 2017: The Olympic
- 924 Mountains Experiment (OLYMPEX). Bull. Amer. Meteor. Soc., 98, 2167-2188.

925

- 926 Hubbert, J. C., V. N. Bringi, and D. Brunkow, 2003: Studies of thepolarimetric
- 927 covariance matrix. Part I: Calibration method-ology.J. Atmos. Oceanic
- 928 Technol., 20, 696-706.

930 Internet Movie Database, 2011: Tornado Alley. 931 Junyent, F., V. Chandrasekar, D. McLaughlin, E. Insanic, N. Bharadwaj, 2010: The 932 CASA Integrated Project 1 Networked Radar System, J. Atmos. Ocean, Tech., 27, 61-933 78. 934 935 Keeler, R. J., B. W. Lewis, and G. R. Gray, 1989: Description of NCAR/FOF CP-2 936 meteorological Doppler radar. Preprints, 24th Conf. on Radar Meteorology, 937 938 Tallahassee, FL, Amer. Meteor. Soc., 589–592. 939 Keeler, R. J., and C. L. Frush, 1983: Rapid scan Doppler radar development 940 considerations, Part II: Technology Assessment. Preprints, 21st Conf. on Radar 941 Meteorology, Edmonton, Canada, Amer. Meteor. Soc., 284-290. 942 943 944 Kosiba, K. A., 2009: A comparison of radar observations to real data simulations of axisymmetric tornadoes. Ph.D. dissertation, Department of Earth and Atmospheric 945 Sciences, Purdue University, 126pp. 946 947 Kosiba, K. A. and J. Wurman 2009. High resolution and in-situ observations in the 948 hurricane boundary layer: Ike and Gustav. 34th Conference on Radar Meteorology, 949 Williamsburg, VA, Amer. Meteor. Soc., 950 https://ams.confex.com/ams/34Radar/webprogram/Paper156151.html 951 952

- 953 Kosiba, K., and J. Wurman, 2010: The Three-Dimensional Axisymmetric windfield Structure of the Spencer, South Dakota, 1998 Tornado. J. Atmos. Sci., 67, 3074-3083. 954 955 Kosiba, K. A. and co-authors, 2012. Mobile radar observations and damage 956 957 assessment of the 24 May 2011, Canton Lake, OK tornado. 26th Conference on Severe Local Storms, Nashville, TN, Amer. Meteor. Soc., 958 https://ams.confex.com/ams/26SLS/webprogram/Paper211754.html 959 960 961 Kosiba, K., J. Wurman, 2013: The three-dimensional structure and evolution of a tornado boundary layer. Wea. and Forecasting, 28, 1552-1561. 962 963 Kosiba, K., J. Wurman, F. J. Masters, and P. Robinson, 2013: Mapping of near-surface 964 winds in Hurricane Rita using fine-scale radar, anemometer and land-use data. Mon. 965
- 967

- Kosiba, K., J. Wurman, Y. Richardson, P. Markowski, P. Robinson, and J. Marquis,
- 2013b: Genesis of the Goshen County, Wyoming, Tornado on 5 June 2009 during
- 970 VORTEX2. Mon. Wea. Rev., 141, 1157-1181.

Wea. Rev., 141, 4337-4349.

- 971
- 972 Kosiba, K.A., J. Wurman, 2014: Fine-scale dual-Doppler analysis of hurricane
- boundary layer structures in Hurricane Frances (2004) at landfall. *Mon. Wea. Rev.*,
- 974 **142**, 1874-1891.

- Kosiba, K. A. and J. Wurman 2016: The TWIRL (Tornado Winds from In-situ and
- Project. 28th Conference on Severe Local Storms, Portland, OR,
- 978 Amer. Meteor. Soc.,
- 979 https://ams.confex.com/ams/28SLS/webprogram/Paper302011.html

- Kosiba, K. A. and J. Wurman 2016: PECAN: Characteristics of Potentially Severe
- Wind Producing Nocturnal MCSs. 98th AMS Annual Meeting, Austin, TX, Amer. Meteor.
- 983 Soc., https://ams.confex.com/ams/98Annual/webprogram/Paper335012.html

984

- Kosiba, K. A., and J. Wurman 2018: Mapping of Winds in Landfalling Irma from Two
- DOWs and Several Pods Deployed Near Naples, Florida. 33rd Conference on
- 987 Hurricanes and Tropical Meteorology, Ponte Verda, FL, Amer. Meteor. Soc.,
- https://ams.confex.com/ams/33HURRICANE/webprogram/Paper340238.html
- Kosiba, K.A., J. Wurman, K. Knupp, K. Pennington, and P. Robinson, 2020: Ontario
- 990 Winter Lake-effect Systems (OWLeS): Bulk Characteristics and Kinematic Evolution of
- 991 Misovortices in Long-Lake-Axis-Parallel Snowbands. *Mon. Wea. Rev.*, **148**, 131–157.

- 993 Kosiba, K. A., Wurman, J., and P. Robinson, 2020b: Low-Level Winds in
- 994 Tornadoes. Severe Local Storms Symposium, 100th AMS Annual Meeting. Boston,
- 995 MA, Amer. Meteor. Soc.,
- 996 https://ams.confex.com/ams/2020Annual/meetingapp.cgi/Paper/369823

- 998 Kristovich, D., R. Clark, J. Frame, B. Geerts, K. Knupp, K. Kosiba, N. Laird, N. Metz, J.
- 999 Minder, T. Sikora, W. Steenburgh, S. Steiger, J. Wurman, and G. Young, 2017: The
- 1000 Ontario Winter Lake-Effect Systems Field Campaign: Scientific and Educational
- Adventures to Further Our Knowledge and Prediction of Lake-Effect Storms. *Bull.*
- 1002 Amer. Meteor. Soc., **98**, 315–332

- Kumjian, M. R., and A. V. Ryzhkov, 2008: Polarimetric signatures in supercell
- thunderstorms. Journal of Applied Meteorology and Climatology, **47**, 1940–1961.

1006

- Lee, W.-C., and J. Wurman, 2005: Diagnosed Three-Dimensional Axisymmetric
- 1008 Structure of the Mulhall Tornado on 3 May 1999. *J. Atmos. Sci.*, **62**, 2373-2393.

1009

- Lee, J. L., Samaras, T., and C. Young, 2004: Pressure measurements at the ground in
- an F-4 tornado. 22nd Conference on Severe Local Storms. Hyannis, MA, Amer.
- 1012 Meteor. Soc.,
- https://ams.confex.com/ams/11aram22sls/techprogram/paper 81700.htm

- Lee, W.-C., F. D. Marks, and R. E. Carbone, 1994: Velocity Track Display—A
- technique to extract real-time tropical cyclone circulations using a single airborne
- Doppler radar. J. Atmos. Oceanic Technol., 11, 337–356.

- Lorsolo, S., J. L. Schroeder, P. Dodge, and F. Marks, 2008: An observational study of
- hurricane boundary layer small-scale coherent structures. *Mon. Wea. Rev.*, **136**, 2871–
- 1020 2893.
- Lutz, J., P. Johnson, B. Lewis, E. Loew, M. Randall, and J. VanAndel, 1995: NCAR's
- S-POL portable polarimetric C-band radar. Preprints, Ninth Symp. on Meteorological
- 1023 Observations and Instrumentation, Charlotte, NC, Amer. Meteor. Soc., 408–410.
- Maddox, R. A., J. Zhang, J. J. Gourley, and K. W. Howard, 2002: Weather Radar
- 1025 Coverage over the Contiguous United States, *Wea. Forecasting*, **17**, 927-934.
- Markowski, P. M., J. M. Straka, and E. N. Rasmussen, 2002: Direct Surface
- 1027 Thermodynamic Observations within the Rear-Flank Downdrafts of Nontornadic and
- 1028 Tornadic Supercells, *Mon. Wea. Rev.*, **130**, 1692-1721.
- 1029
- Markowski, P., Y. Richardson, J. Marquis, J. Wurman, K. Kosiba, P. Robinson, D.
- Dowell, E. Rasmussen, R. Davies-Jones, 2012a: The Pretornadic Phase of the
- Goshen County, Wyoming, Supercell of 5 June 2009 Intercepted by VORTEX2. Part I:
- Evolution of Kinematic and Surface Thermodynamic Fields. *Mon. Wea. Rev.*, **140**,
- 1034 2887-2915.
- 1035
- Markowski P., Y. Richardson, J. Marguis, R. Davies-Jones, J. Wurman, K. Kosiba, P.
- Robinson, E. Rasmussen, D. Dowell, 2012b: The Pretornadic Phase of the Goshen
- 1038 County, Wyoming, Supercell of 5 June 2009 Intercepted by VORTEX2. Part II:
- 1039 Intensification of Low-Level Rotation. *Mon. Wea. Rev.*, **140**, 2916-2938.

1040	
1041	Markowski, P.M., T. P. Hatlee, and Y. P. Richardson, 2018: Tornadogenesis in the 12
1042	May 2010 Supercell Thunderstorm Intercepted by VORTEX2 near Clinton, Oklahoma.
1043	Mon. Wea. Rev., 146 , 3623–3650.
1044	
1045	Markowski, P. M., Y. P. Richardson, S. J. Richardson, and A. Petersson, 2018: Above-
1046	ground thermodynamic observations in convective storms from balloon-borne probes
1047	acting as pseudo-Lagrangian drifters. Bull. Amer. Meteor. Soc., 99, 711–724
1048	Marquis, J.N., Y.P. Richardson, J.M. Wurman, 2007: Kinematic Observations of
1049	Misocyclones along Boundaries during IHOP. Mon. Wea. Rev., 135, 1749-1768.
1050	
1051	Marquis, J., Y. Richardson, J. Wurman, P. Markowski, 2008: Single- and Dual-Doppler
1052	Analysis of a Tornadic Vortex and Surrounding Storm-Scale Flow in the Crowell,
1053	Texas, Supercell of 30 April 2000. Mon. Wea. Rev., 136, 5107-5043.
1054	
1055	Marquis, J., Y. Richardson, P. Markowski, D. Dowell, J. Wurman, 2012: Tornado
1056	Maintenance Investigated with High-Resolution Dual-Doppler and EnKF Analysis, Mon.
1057	Wea. Rev., 140 , 3-27.
1058	
1059	Marshall, J. S., and W. McK. Palmer, 1948: The distribution of raindrops with size. <i>J.</i>
1060	Meteor., 5 , 165–166.
1061	

- Masters, F.J., H. W. Tieleman, and J. A. Balderrama, 2010: Surface wind
- measurements in three gulf coast hurricanes of 2005. Journal of Wind Engineering and
- 1064 Industrial Aerodynamics, 98, 533-547.
- Miller, R.L., C.L. Ziegler, M.I. Biggerstaff, 2020: Seven-Doppler Radar and In-Situ
- Analysis of the 25-26 June 2015 Kansas MCS during PECAN. Mon. Wea. Rev., 148,
- 1067 211-240.

- Milrad, S. and C. Herbster, 2017: Mobile Radar as an Undergraduate Education and
- 1070 Research Tool: The ERAU C-BREESE Field Experience with the Doppler-on-Wheels.
- 1071 Bull. Amer. Meteor. Soc., 98, 1931-1948.

1072

- Morrison, I., S. Businger, F. Marks, P. Dodge, and J. A. Businger 2005: An
- Observational Case for the Prevalence of Roll Vortices in the Hurricane Boundary
- 1075 Layer, *J. Atmos. Sci.*, **62**, 2662-2673.

- Mueller, S., C. S. Morse, D. Garvey, R. Barron, D. Albo and P. Prestopnik, 2004:
- Juneau airport wind hazard alert system display products. 11th Conference on
- 1079 Aviation, Range, and Aerospace Meteorology, Hyannis, MA, Amer. Meteor. Soc.,
- https://ams.confex.com/ams/11aram22sls/techprogram/paper_81647.htm
- Mulholland, J.P., J. Frame, S.W. Nesbitt, S.M. Steiger, K.A. Kosiba, and J. Wurman,
- 2017: Observations of Misovortices within a Long-Lake-Axis-Parallel Lake-Effect
- 1083 Snowband during the OWLeS Project. *Mon. Wea. Rev.*, **145**, 3265-3291.

National Science Foundation (NSF) 2015: Mission impossible? New England's 1085 snowstorm 'bomb' from inside a Doppler-on-Wheels. Research News. Accessed 12 1086 January 2021. https://www.nsf.gov/discoveries/disc_summ.jsp?cntn_id=134156 1087 1088 National Severe Storms Lab (NSSL), 2021: Research Tools: Mobile 1089 Radar. Accessed 12 January 2021, https://www.nssl.noaa.gov/tools/radar/mobile/ 1090 1091 1092 Nesbitt, S. N, P. V. Salio, E. Ávila, P. Bitzer, L. Carey, V. Chandrasekar, W. Deierling, F. Dominguez, M. E. Dillon, C. M. Garcia, D. Gochis, S. Goodman, D. A. Hence, K. A. 1093 Kosiba, M. R. Kumjian, T. Lang, J. Marquis, R. Marshall, L. A. McMurdie, E. L. 1094 1095 Nascimento, K. L. Rasmussen, R. Roberts, A. K. Rowe, J. J. Ruiz, E. F.M.T. São Sabbas, A. C. Saulo, R. S. Schumacher, Y. G. Skabar, L. A. T. Machado, R. J. Trapp, 1096 A. Varble, J. Wilson, J. Wurman, E. J. Zipser, I. Arias, H. Bechis, and M. A. Grover, 1097 2021: A storm chasing safari in Subtropical South America: proyecto 1098 RELAMPAGO. Bull. Amer. Meteor. Soc., in review. 1099 1100 Niziol, T. A., W. R. Snyder, and J. S. Waldstreicher, 1995: Winter weather forecasting 1101 throughout the eastern United States. Part IV: Lake-effect snow. Wea. Forecasting, 10, 1102 1103 61–77.

1104 Office of the Federal Coordinator for Meteorological Services and Supporting Research (OFCM) 2017: WSR-88D Meteorological Observations. Accessed 12 January 2021, 1105 https://www.icams-portal.gov/publications/fmh/FMH11/fmh11partC.pdf 1106 1107 Pazmany, A. L., J. B. Mead, H. B. Bluestein, , J. C. Snyder, , and J. B. Houser, 2013: A 1108 mobile rapid-scanning X-band polarimetric (RaXPol) Doppler radar system. J. Atmos. 1109 Oceanic Technol., 30, 1398–1413. 1110 1111 Petersen, W.A., K. Knupp, J. Walters, W. Deierling, M. Gauthier, B. Dolan, J.P. Dice, 1112 1113 D. Satterfield, C. Davis, R. Blakeslee, S. Goodman, S. Podgorny, J. Hall, M. Budge, A. Wooten, 2004: The UAH-NSSTC/WHNT ARMOR C-band dual-polarimetric radar: a 1114 unique collaboration in research, education and technology transfer, Preprints, 32nd 1115 Conf. on Radar Meteor., Amer. Meteor. Soc., Albuquerque, New Mexico, 12R.4 1116 1117 1118 Petersen, W.A., and D. B. Wolff, 2013: The NASA Polarimetric Radar (NPOL). Accessed 12 January 2021, 1119 1120 https://ntrs.nasa.gov/archive/nasa/casi.ntrs.nasa.gov/20140010713.pdf 1121 Protat, A., and I. Zawadzki, 1999: A variational method for real-time retrieval of three-1122 dimensional windfield from multiple-Doppler bistatic radar network data. J. Atmos. 1123 Oceanic Technol., 16, 432-449. 1124

- Ralph, F. M. and coauthors, 1999: The California Land-falling Jets Experiment
- 1127 (CALJET): Objectives and Design of a Coastal Atmosphere-Ocean Observing System
- Deployed During a Strong El Nino. Preprints, 3rd Symposium on Integrated Observing
- 1129 Systems, Dallas, TX, Amer. Meteor. Soc., p. 78-81.

- Rappin, E., R. Mahmood, U. Nair, R. A. Pielke Sr., W. Brown, S. Oncley, J. Wurman, K.
- Kosiba, A, Kaulfus, C. Phillips, E. Lachenmeier, J. Santanello Jr., E. Kim, and P.
- Lawston-Parker, 2021: The Great Plains Irrigation Experiment (GRAINEX). Bull. Amer.
- 1134 Meteor. Soc., Accepted pending revisions.

1135

- Rasmussen, E. N., J. M. Straka, R. Davies-Jones, C. A. Doswell III, F. H. Carr, M. D.
- Eilts, and D. R. MacGorman, 1994: Verification of the Origins of Rotation in Tornadoes
- Experiment: VORTEX. Bull. Amer. Meteor. Soc., 75, 995-1006.

1139

- Rauber, R. M., and S.W. Nesbitt, 2018: *Radar Meteorology: A First Course*. John
- 1141 Wiley & Sons, 166pp.

1142

- Ray, P. S., R. J. Doviak, G. B. Walker, D. Sirmans, J. Carter, and B. Bumgarner, 1975:
- Dual-Doppler Observation of a Tornadic Storm, J. Appl. Meteor. Climatol., 14, 1521-
- 1145 1530.

- 1147 Refan, M., H. Hangan, J. Wurman, 2014: Reproducing tornadoes in laboratory using
- proper scaling. J. Wind Engineering and Industrial Aerodynamics, 135, 136-148.

1171 Schroeder, J. L., and C. C. Weiss, 2008: Integrating research and education through measurement and analysis. Bull. Amer. Meteor. Soc., 89, 793-804. 1172 1173 1174 Schultz, D.M., and Coauthors, 2002: Understanding Utah Winter Storms: The Intermountain Precipitation Experiment. Bull. Amer. Meteor. Soc., 83, 189-210. 1175 1176 Schumacher, R., D. A. Hence, S. W. Nesbitt, R. J. Trapp, K. A. Kosiba, J. Wurman, P. 1177 Salio, M. Runga, A. Varble, N. R. Kelly, 2021: Convective-storm environments in 1178 subtropical South America from high-frequency soundings during RELAMPAGO-1179 CACTI. Mon. Wea. Rev., Accepted, pending revisions. 1180 1181 Shapiro, A., C. K. Potvin, and J. Gao, 2009: Use of a vertical vorticity equation in 1182 variational dual-Doppler wind analysis. J. Atmos. Oceanic Technol., 26, 2089–2106. 1183 1184 1185 Steiger, S. A., D. Stamm, K. Ruth, T. Jaszka, B. Kress, R. Rathbun, J. Schrom, J. 1186 Frame, J. Wurman, and K. Kosiba, 2013: Circulations, Bounded Weak Echo Regions, 1187 and Horizontal Vortices Observed by the Doppler on Wheels during Long Lake-Axis-1188 Parallel Lake-effect Storms over Lake Ontario During the Winter of 2010-11. *Mon.* Wea. Rev., 141, 2821-2840. 1189 1190

- 1191 Straka, J. M., E. N. Rasmussen, and S. E. Fredrickson, 1996: A mobile mesonet for
- finescale meteorological observations. *J. Atmos. Oceanic Technol.*, **13**, 921–936.

- Stout, G. E., and F. A. Huff, 1953: Radar records Illinois tornadogenesis. *Bull. Amer.*
- 1195 *Meteor. Soc.*, **34**, 281–284.

1196

- 1197 Tessendorf, S.A., J.R. French, K. Friedrich, B. Geerts, R.M. Rauber, R.M. Rasmussen,
- L. Xue, K. Ikeda, D.R. Blestrud, M.L. Kunkel, S. Parkinson, J.R. Snider, J. Aikins, S.
- Faber, A. Majewski, C. Grasmick, P.T. Bergmaier, A. Janiszeski, A. Springer, C.
- 1200 Weeks, D.J. Serke, and R. Bruintjes, 2019: A Transformational Approach to Winter
- Orographic Weather Modification Research: The SNOWIE Project. *Bull. Amer. Meteor.*
- 1202 *Soc.*, **100**, 71–92.
- 1203 Toth, M., E. Jones, D. Pittman, D. Solomon, 2011: DOW Radar Observations of Wind
- 1204 Farms. Bull. Amer. Met. Soc., **92**, 987-995.
- Toth, M., R.J. Trapp, J. Wurman, K. Kosiba, 2013: Comparison of Mobile-Radar
- Measurements of Tornado Intensity with Corresponding WSR-88D Measurements.
- 1207 Wea. and Forecasting, **28**, 418-426.

1208

- 1209 Trapp, R. J., 2013: Mesoscale-Convective Processes in the Atmosphere. Cambridge
- 1210 University Press, 346 pp.

- 1212 Trapp, R. J., Stensrud, D. J., Coniglio, M. C., Schumacher, R. S., Baldwin, M. E.,
- Waugh, S., & Conlee, D. T., 2016: Mobile Radiosonde Deployments during the
- Mesoscale Predictability Experiment (MPEX): Rapid and Adaptive Sampling of Upscale
- 1215 Convective Feedbacks, Bull. Amer. Meteor. Soc., 97, 329-336.

- 1217 Trapp, J., Hence, D., Kosiba, K., Kumjian, M., Marquis, J., Nesbitt, S., P. Salio, and J.
- 1218 Wurman, 2020: Multiple-platform, and multiple-Doppler radar observations of a
- supercell thunderstorm in South America during RELAMPAGO. *Mon. Wea. Rev.*, 148,
- 1220 3225 3241.

1221

- 1222 University of Alabama Huntsville (UAH), 2021. MAX (Mobile Alabama X-Band).
- Accessed on 12 January 2021, https://www.nsstc.uah.edu/mips/max/

1224

- Wakimoto, R.M., N.T. Atkins, J. Wurman, 2011: The LaGrange Tornado during
- VORTEX2. Part I: Photogrammetric Analysis of the Tornado Combined with Single-
- 1227 Doppler Radar Data. *Mon. Wea. Rev.*, 139, 2233-2258.

1228

- Wakimoto, R.M., P. Stauffer, W.-C. Lee, N.T. Atkins, J. Wurman, 2012: Finescale
- 1230 Structure of the LaGrange, Wyoming, Tornado during VORTEX2: GBVTD and
- 1231 Photogrammetric Analyses. *Mon. Wea. Rev.*, 140, 3397-3418.

- Weckwerth, T.M., T.W. Horst, J.W. Wilson, 1999: An Observational Study of the
- Evolution of Horizontal Convective Rolls. *Mon. Wea. Rev.*, 127, 2160-2179.

- Weckwerth, T. M., L. J. Bennett, L. J. Miller, J. V. Baelen, P. D. Girolamo, A. M. Blyth,
- 1236 T. J. Hertneky, 2014: An Observational and Modeling Study of the Processes Leading
- to Deep, Moist Convection in Complex Terrain, Mon. Wea. Rev., 142, 2687-2708.

- Wakimoto, R. M., and V. N. Bringi, 1988: Dual-polarization observations of microbursts
- associated with intense convection: The 20 July storm during the MIST Project. Mon.
- 1241 Wea. Rev., **116**, 1521-1539.

1242

1243

- Weiss, C. C., J. L. Schroeder, J. Guynes, P. S. Skinner, and J. Beck, 2009: The
- 1245 TTUKa mobile Doppler radar: Coordinated radar and in-situ measurements of supercell
- thunderstorms during Project VORTEX2. 34th Conf. on Radar Meteorology,
- 1247 Williamsport, VA, Amer. Meteor. Soc.,
- https://ams.confex.com/ams/34Radar/techprogram/paper 155425.htm

1249

- Wilson, J. W., R. D. Roberts, C. Kessinger, J. McCarthy, 1984: Microburst Wind
- Structure and Evaluation of Doppler Radar for Airport Wind Shear Detection. *J. Appl.*
- 1252 *Meteor. Climatol.*, **23**, 898-915.
- 1253 Wilson, J. W., and W. E. Schreiber, 1986: Initiation of convective storms at radar-
- observed boundary-layer convergence lines. *Mon. Wea. Rev.*, **114**, 2516–2536.

Winn, W. P., S. J. Hunyady, and G. D. Aulich, 1999: Pressure at the ground in a large 1256 tornado, J. Geophys. Res., 104, 22067-22082. 1257 1258 Wulfmeyer, V. et al., 2008: Research Campaign: The Convective and Orographically 1259 Induced Precipitation Study. Bull. Amer. Meteor. Soc., 89, 1477-1486. 1260 1261 Wurman, J., S. Heckman, and D. Boccippio, 1993: A bistatic multiple-Doppler network. 1262 J. Appl. Meteor. Climatol., 32, 1802-1814. 1263 1264 Wurman, J., 1994: Vector winds from a single transmitter bistatic dual-Doppler radar 1265 network, Bull. Amer. Meteor. Soc., 75, 983-994. 1266 1267 Wurman, J., J. Straka, E. Rasmussen, 1996: Fine Scale Doppler Observation of 1268 Tornadoes. Science, 272, 1774-1777. 1269 1270 Wurman, J., J. Straka, E. Rasmussen, M. Randall, and A. Zahrai, 1997: Design and 1271 Deployment of a Portable, Pencil-Beam, Pulsed, 3-cm Doppler Radar. J. Atmos. 1272 Oceanic Tech., 14, 1502-1512. 1273 1274 Wurman, J., and J. Winslow, 1998: Sub-Kilometer-Scale Boundary Layer Rolls. 1275

Science, 280, 555-557.

1276

Wurman, J., S. Gill, 2000: Finescale Radar Observations of the Dimmitt, Texas (2 June 1278 1995), Tornado. Mon, Wea Rev., 128, 2135-2164. 1279 1280 Wurman, J., and M. Randall, 2001: An inexpensive, mobile, rapid-scan radar. 30th 1281 Conference on Radar Meteorology, Munich, Germany, Amer. Meteor. 1282 Soc., https://ams.confex.com/ams/30radar/techprogram/paper 21577.htm 1283 1284 1285 Wurman, J., 2002: The Multiple-Vortex Structure of a Tornado. Wea. and Forecasting, 1286 **17**, 473-505. 1287 Wurman, J., 2003 Multiple-Doppler Observations of tornadoes and tornadogenesis 1288 from the ROTATE-2003 project. 31st Conference on Radar Meteorology, Seattle, WA, 1289 Amer. Meteor. Soc., 1290 https://ams.confex.com/ams/32BC31R5C/webprogram/Paper63886.html 1291 1292 Wurman, J. and S. Weygandt, 2003: Mobile Radar Observations of the Big Elk (2002) 1293 and Roberts (2003) Fires. 5th Symposium on Fire and Forest Meteorology. Orlando, 1294 FL, Amer. Meteor. Soc., 1295 https://ams.confex.com/ams/FIRE2003/techprogram/paper 65727.htm 1296 1297 Wurman, J., 2004. High Resolution Observations of Boundary Layer Structures in 1298

Isabel at Landfall. 26th Conference on Hurricanes and Tropical Meteorology. Miami,

1300 FL, Amer. Meteor. Soc., https://ams.confex.com/ams/26HURR/webprogram/Paper76440.html 1301 1302 1303 Wurman, J., and T. Samaras, 2004: Comparison of in-situ pressure and DOW Doppler winds in a tornado and RHI vertical slices through 4 tornadoes during 1996-1304 2004. 22nd Conference on Severe Local Storms. Hyannis, MA, Amer. Meteor. Soc., 1305 https://ams.confex.com/ams/11aram22sls/techprogram/paper 82352.htm 1306 1307 Wurman, J., C.R. Alexander, 2005: The 30 May 1998 Spencer, South Dakota, Storm. 1308 Part II: Comparison of Observed Damage and Radar-Derived Winds in the Tornadoes. 1309 Mon. Wea. Rev., 133, 97-119. 1310 Wurman, J., Y. Richardson, C. Alexander, S. Weygandt, P.F. Zhang, 2007a: Dual-1311 Doppler and Single-Doppler Analysis of a Tornadic Storm Undergoing Mergers and 1312 1313 Repeated Tornadogenesis. Mon. Wea. Rev., 135, 736-758. 1314 Wurman, J., Y. Richardson, C. Alexander, S. Weygandt, P.F. Zhang, 2007b: Dual-1315 1316 Doppler Analysis of Winds and Vorticity Budget Terms near a Tornado. Mon. Wea. Rev., 135, 2392-2405. 1317

1318 Wurman, J., P. Robinson, C. Alexander, Y. Richardson, 2007c: Low-Level Winds in Tornadoes and Potential Catastrophic Tornado Impacts in Urban Areas. Bull. Amer. 1319 Meteor. Soc., 88, 31-46. 1320 1321 Wurman, J., 2008: Preliminary Results and Report of the ROTATE-2008 radar / in-situ 1322 / mobile mesonet experiment. 24th Conference on Severe Local Storms. Savannah, 1323 GA, Amer. Meteor. Soc., 1324 https://ams.confex.com/ams/24SLS/webprogram/Paper142200.html 1325 1326 Wurman, J., K. Kosiba, P. Markowski, Y. Richardson, D. Dowell, and P. Robinson, 1327 2010: Finescale Single- and Dual-Doppler Analysis of Tornado Intensification, 1328 1329 Maintenance, and Dissipation in the Orleans, Nebraska, Supercell. Mon. Wea. Rev., **138**, 4439-4455. 1330 1331 Wurman, J., D. Dowell, Y. Richardson, P. Markowski, E. Rasmussen, D. Burgess, L. 1332 Wicker, and H.B. Bluestein 2012: The Second Verification of the Origins of Rotation in 1333 Tornadoes Experiment: VORTEX2. Bull. Amer. Meteor. Soc., 93, 1147-1170. 1334 1335 1336 Wurman, J., K. Kosiba, 2013: Finescale Radar Observations of Tornado and Mesocyclone Structures. Wea. and Forecasting, 28, 1157-1174. 1337

1339	Wurman, J., K. Kosiba, P. Robinson, 2013a: In-Situ, Doppler Radar, and Video
1340	Observations of the Interior Structure of a Tornado and the Wind-Damage
1341	Relationship. Bull. Amer. Meteor. Soc., 94, 835-846.
1342	
1343	Wurman, J. K. Kosiba, and P. Robinson, 2013b: Wind Speed Suppression by Large
1344	Buildings in Hurricanes. 36th Conference on Radar Meteorology. Breckenridge, CO,
1345	Amer. Meteor.
1346	Soc., https://ams.confex.com/ams/36Radar/webprogram/Paper229320.html
1347	
1348	Wurman, J. K. Kosiba, P. Robinson, and F. J. Masters, 2013c: Fine-scale dual-
1349	Doppler and in-situ observations of the boundary layer in Hurricane Isaac. 36th
1350	Conference on Radar Meteorology. Breckenridge, CO, Amer. Meteor. Soc.,
1351	https://ams.confex.com/ams/36Radar/webprogram/Paper229319.html
1352	
1353	Wurman, J., K.A. Kosiba, P. Robinson, T. Marshall, 2014: The Role of Multiple Vortex
1354	Tornado Structure in Causing Storm Researcher Fatalities. Bull. Amer. Meteor. Soc.,
1355	95 , 31-45.
1356	
1357	Wurman, J., and co-authors, 2016. Very Fine-Scale Dual-Doppler and In-Situ Analysis
1358	of a Strong Tornado. 28th Conference on Severe Local Storms, Portland, OR, Amer.
1359	Meteor. Soc., https://ams.confex.com/ams/28SLS/webprogram/Paper302005.html
1360	

1361	Wurman, J. and K. Kosiba, 2018: The role of small-scale vortices in enhancing surface
1362	winds and damage in Hurricane Harvey (2017). Mon. Wea. Rev., 146, 3441-3463.
1363	
1364	Wurman and Kosiba 2018: Fine-Scale Multiple-Doppler and Thermodynamic
1365	Observations in an Eclipse. 98th AMS Annual Meeting, Austin, TX, Amer. Meteor.
1366	Soc.,
1367	https://ams.confex.com/ams/98Annual/webprogram/Paper340290.html
1368	
1369	Wurman, J., K. A. Kosiba, T. White, P. Robinson, 2021: Supercell Tornadoes are
1370	Much Stronger and Wider than Damage-Based Ratings Indicate. PNAS, 188 (14),
1371	e2021535118; https://doi.org/10.1073/pnas.2021535118.
1372	
1373	Ziegler, C. L., M. S. Buban, and E. N. Rasmussen, 2007: A Lagrangian Objective
1374	Analysis Technique for Assimilating In-Situ Observations with Multiple-Radar-Derived
1375	Airflow. Mon. Wea. Rev., 135 , 2417-2442.

1377 Table 1: FARM radar specifications

Basic Specs	DOW1	DOW2,3	DOW 6,7	cow	DOW 8	RSDOW
Tx kW peak	40	250	2x 250	2x 1000	100	40
PRF Hz	500-2000 (later 500- 4000) w/stagger	500-5000 w/stagger	500-6000 w/stagger			
Pulse Length □s	0.5 - 1.0 (later 0.25-1)	0.167 - 1.0	0.167-1.0 s 0.1-1.0 s			0.1-1.0 s
Scan rate °/s	30 (later 50)	50	50	24 °/s	50	7-s vols
Products	Z,V,NCP, SW	Z,V,NCP,SW	LDR, ZDR, Rho- HV, V, Z, SW, NCP, IQ		Z,V,SW,NCP, IQ	
Beamwidth °	1.22 (later 0.93)	0.93	0.93	1.05	0.93	0.8x0.9
Gate Length m	75-300 (later 25-300)	12.5-600	12.5-600 m		11-600	
Meteorological and Comm Mast	none	10 m	18 m	future mast	14 m	

Table 2: Farm in-situ instrument specifications.

	PODNET	POLENET	Mobile Mesonet	Upper Air Soundings	Disdromete rs
Number	Up to 20	3-12 (can share instrumentation package with PodNet)	3	6 Graw 1 Windsond/S warmsonde	4
Measurements	T/RH (Campbell Scientific EE181- L/Rotronic HC2S3 + Shield RAD10E), P (Vaisala PTB1100), GPS (Garmin 16X- HVS), Wind x 2 (RM Young Jr. 04101 and Gill WindSonic 75 Ultrasonic)	can be customized with any	T/RH (Campbell Scientific EE181-L + Shield) P (Vaisala PTB1100), GPS (Garmin 16X- HVS), Wind (RM Young 05103) Can host others.	T, RH, Wind, P	Drop Size Distribution
Sampling Rate	Up to 10 Hz	Up to 10 Hz	Up to 10 Hz	1 s	10 s
Real-time Data	yes	yes	yes	yes	no
Platform	Hardened steel "T" stand	Attaches to infrastructure such as power and light poles, railings, at user specified heights	sounding systems;	Graw Windsonic	OTT Parsivel
Height	Configurable (currently 1, 1.5, 2 m)	Configurable, on existing infrastructure. Typically 3-10 m	3.5 m	1-20000 m	1 m
Camera/Video Attachment	yes	yes	yes	no	yes
Comm Compatibility	Cellular Internet	Cellular Internet	Cellular Internet		
Data	local	local or wireless	local or internet	local	local

Figure Caption List

1385

1386

1387

1388

1389

1390

1391

1392

1393

1394

1395

1396

1397

1398

1399

1400

1401

1402

1384

Figure 1. What Radars Can and Cannot Resolve. 1/4 scales (diameters) of phenomena compared to radar observing scales (logarithmic axes) reveal whether radars can well-resolve various phenomena. For example, to well-resolve a 10 km diameter mesocylone with an ~2000 s temporal scale (duration), observations with scales of < 2.5 km and < 500 s are required. The fraction of the full observing domain achieving given spatial resolutions is illustrated for stationary radars. The spatial scale achieved by MQD DOWs are shown at 2 km and 10 km deployment ranges to observed phenomena. The WSR-88D network can spatially well-resolve large mesocyclones throughout about ½ of its observing domain. But they spatially wellresolve tornadoes over <<1% of their domain and cannot well-resolve tornadoes temporally. Faster-scanning sparse phased array networks could well-resolve tornadoes temporally, but not spatially. Denser arrays of fast-scanning stationary radars, e.g., CASA, would not spatially well-resolve most tornadoes. MQD DOWs can well-resolve many, but not all tornadoes spatially. Rapid-Scanning MQD such as the RSDOW are required to well-resolve rapid tornado evolution, sub-tornado scale vortices, and other rapidly evolving atmospheric phenomena such as turbulent fire plumes, boundary layer eddies, and hurricane tornado-scale vortices.

1403

Figure 2. DOW1 MQD radar in 1995. (From Wurman et al. 1997)

1405

Figure 3. Sample DOW deployments. (a) schematic map of study domains, (b) DOW largely buried in snow at Snowbank, Idaho (2017), (c) DOW observing boundary layer during eclipse (2017), (d) DOW on Cape Cod during Nor'easter (2015), (e) DOW during hurricane Delta (2020) (f) DOW7 cabin interior, (g) DOW observing CalWood fire (2020), (h) Flooded DOW site in Lake Quinault during OLYMPEX (2016), (i) DOW scanning a tornado (2005).

Figure 4. Illustrative FARM data images. (a) Tornadic hook echo, (b) hurricane boundary layer rolls, (c) interior view of hurricane eye with mesovortices, (d) lake-effect snow band misovortices, (e) integrated radar and in-situ observations of a tornado, (f) integrated radar and in-situ observations in a mesoscale convective system, (g) vertical (RHI) slice of microphysical layering during nor'easter, (h) snow bands/cells caused by cloud seeding.

Figure 5. (left) Rapid-Scan DOW (RSDOW) slotted waveguide antenna transmits several simultaneous beams at different elevations using stepped-chirp pulses. Simplified DOW and RSDOW pulse sequences are compared schematically. Mechanical azimuthal scanning rakes the sky at all the elevations, resulting in volumetric data every 7 s. (center) Simultaneous Doppler velocity and Reflectivity slices from different elevations in a tornado. (right) RSDOW with legs and scissor lift extended.

Figure 6. Simplified block diagram of Dual-Frequency Dual-Polarization (DPDF) DOW design. (top) In LDR+45 mode, Frequency 1 (blue paths) is transmitted at horizontal polarization and frequency 2 (green paths) at 45°, permitting LDR calculation. Both frequencies are combined in diplexers, then transmitted and received quasi-simultaneously (black paths) (bottom) Flipping coupled switches enables Fast-45 mode, in which both frequencies are transmitted at 45°, resulting in doubled independent samples, permitting twice-as-fast dual-polarization scanning. Heavy lines indicate "hot" transmission paths. Horizontal and vertical polarization received signals and transmit pulse samples are sent to receivers and signal processors.

Figure 7. C-band vs X-band attenuation, existing MQD radars. Comparison of SR C-band (1.6° beamwidth) and DOW X-band (0.93° beamwidth) observations of a supercell and tornado at about 10 km range to each radar, showing compromises between severe attenuation at X-band and coarse resolution at C-band. Scans are at

Figure 8. COW assembly. COW as transported, antenna being assembled, antenna lifted onto pedestal, deployed

Figure 9. FARM Mobile Mesonets (MM).

approximately 1° elevation.

1452	Figure 10. FARM PODNET units.
1453	
1454	Figure 11. FARM POLENET unit being deployed on power pole during hurricane Delta
1455	(2020).
1456	
1457	Figure 12. FARM MQD sounding being launched from an MM which also carries
1458	PODNET units.
1459	
1460	Figure 13. FARM Mobile Operations and Repair Center (MORC).
1461	
1462	Figure 14. FARM educational and outreach missions. (clockwise from top left) map
1463	of deployments, ad hoc outreach entraining local children to launch upper air
1464	soundings during the GRAINEX field project, DOW at USA Science and Engineering
1465	Festival in Washington DC, university educational deployment, outreach with K-12
1466	children.
1467	
1468	Figure 15. GURU Field Data and Coordination Display. Near real-time imagery from
1469	DOWs/COW is integrated with MM, PODNET, and sounding tracking to aid in mission
1470	planning, radar status, and field coordination. This image is from the real-time GURU
1471	display in the RELAMPAGO operations center. POD and MM locations are shown
1/172	relative to DOW reflectivity and Donnler velocity fields

Figure 16. Comparison of SOWNET and SPOL radar coverage in hypothetical (left)

PECAN- and (center) RICO-type studies. Red and orange circles enclose regions with < 1.7 km beam width (100 km range from S-POL, 67 km range from any of the SOWs). SOWNET provides greater surveillance area. Much of the yellow-shaded areas are within SOWNET multiple-Doppler vector wind coverage. (right) SOW set up requires ~6 hours, much quicker and less expensive than larger S-band radars.

1479

1480

1481

1482

1483

1484

1485

1486

1487

1488

1489

1490

1491

1492

1493

1494

1495

1473

1474

1475

1476

1477

1478

Figure 17. (left) Schematic mobile bistatic network with four receiving antennas and one transmitting radar. The transmitting radar is, in this example, a DOW or SOW, but can be a stationary radar (e.g., S-POL). The four receiving antennas are on the back of pickup trucks, but can be deployed similarly to Pods. The transmitting and receiving radars can be moved like MMs to optimize coverage and vector wind retrievals as phenomena move/evolve. As the DOW/SOW transmits and scans, the pulses in its narrow radar beam (orange arrow) are scattered from hydrometeors, dust, etc. Some of that scattered energy (dashed yellow arrows) is received by the passive antennas, as well as the by the DOW/SOW antenna (dashed orange arrow). Three-dimensional vector wind fields are calculated from these various Doppler measurements. (right) An example of vector wind retrievals from a bistatic network. In this example, there was one transmitting radar (S-POL) and three bistatic receivers (solid squares). The colored vectors depict the retrievals using data from the north (red), central (blue), and southern (green) bistatic receivers. Arcs depict the bistatic dual-Doppler lobes with the transmitting radar. The square outline encloses an overdetermined analysis domain. (Image adapted from Satoh and Wurman 2003).

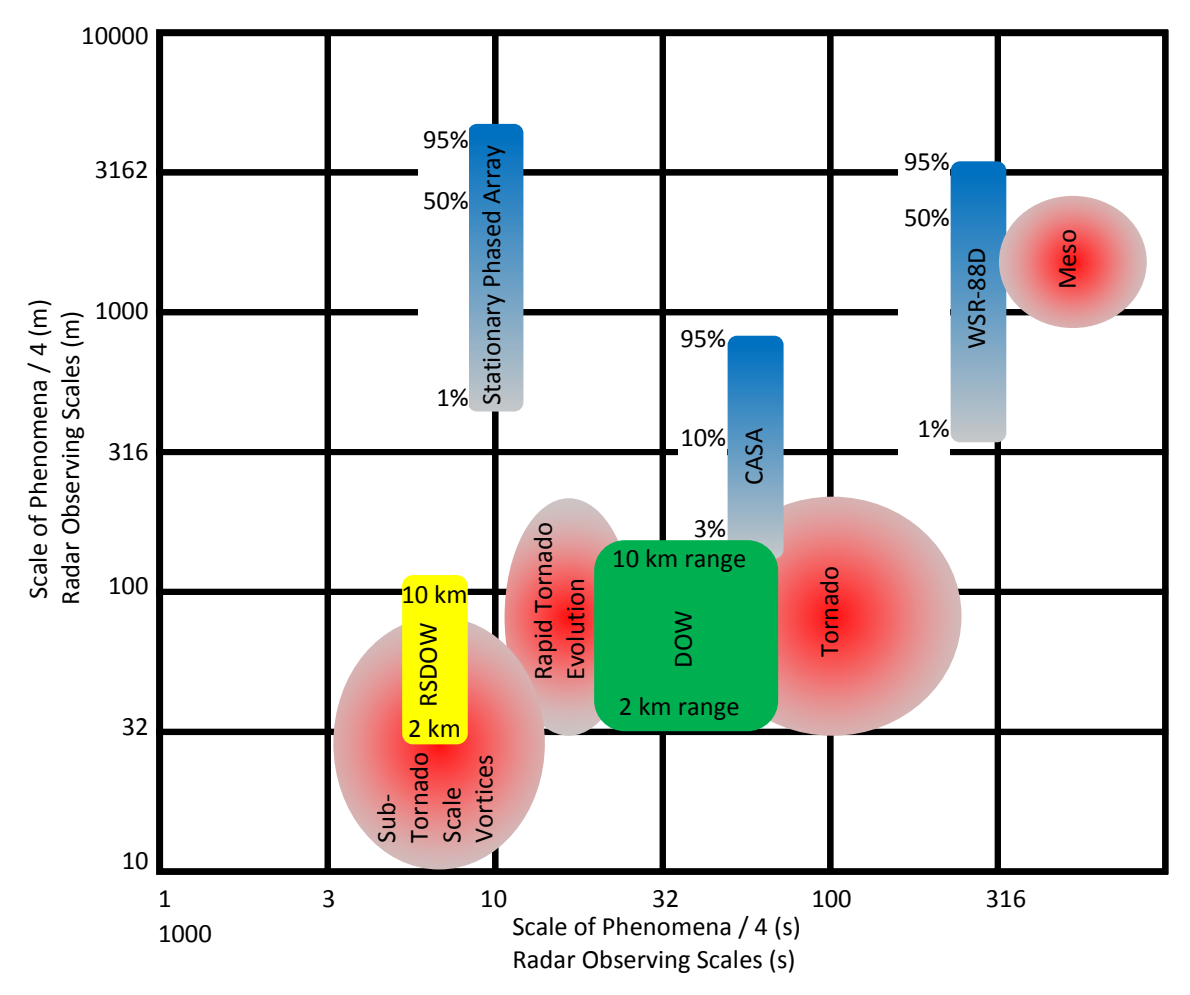


Figure 1. What Radars Can and Cannot Resolve. ¼ scales (diameters) of phenomena compared to radar observing scales (logarithmic axes) reveal whether radars can well-resolve various phenomena. For example, to well- resolve a 10 km diameter mesocylone with an ~2000 s temporal scale (duration), observations with scales of < 2.5 km and < 500 s are required. The fraction of the full observing domain achieving given spatial resolutions is illustrated for stationary radars. The spatial scale achieved by MQD DOWs are shown at 2 km and 10 km deployment ranges to observed phenomena. The WSR-88D network can spatially well-resolve large mesocyclones throughout about ½ of its observing domain. But they spatially well-resolve tornadoes over <<1% of their domain and cannot well-resolve tornadoes temporally. Faster-scanning sparse phased array networks could well-resolve tornadoes temporally, but not spatially. Denser arrays of fast-scanning stationary radars, e.g., CASA, would not spatially well-resolve most tornadoes. MQD DOWs can well-resolve many, but not all tornadoes spatially. Rapid-Scanning MQD such as the RSDOW are required to well-resolve rapid tornado evolution, sub-tornado scale vortices, and other rapidly evolving atmospheric phenomena such as turbulent fire plumes, boundary layer eddies, and hurricane tornado-scale vortices.



Figure 2. DOW1 MQD radar in 1995. (From Wurman et al. 1997)

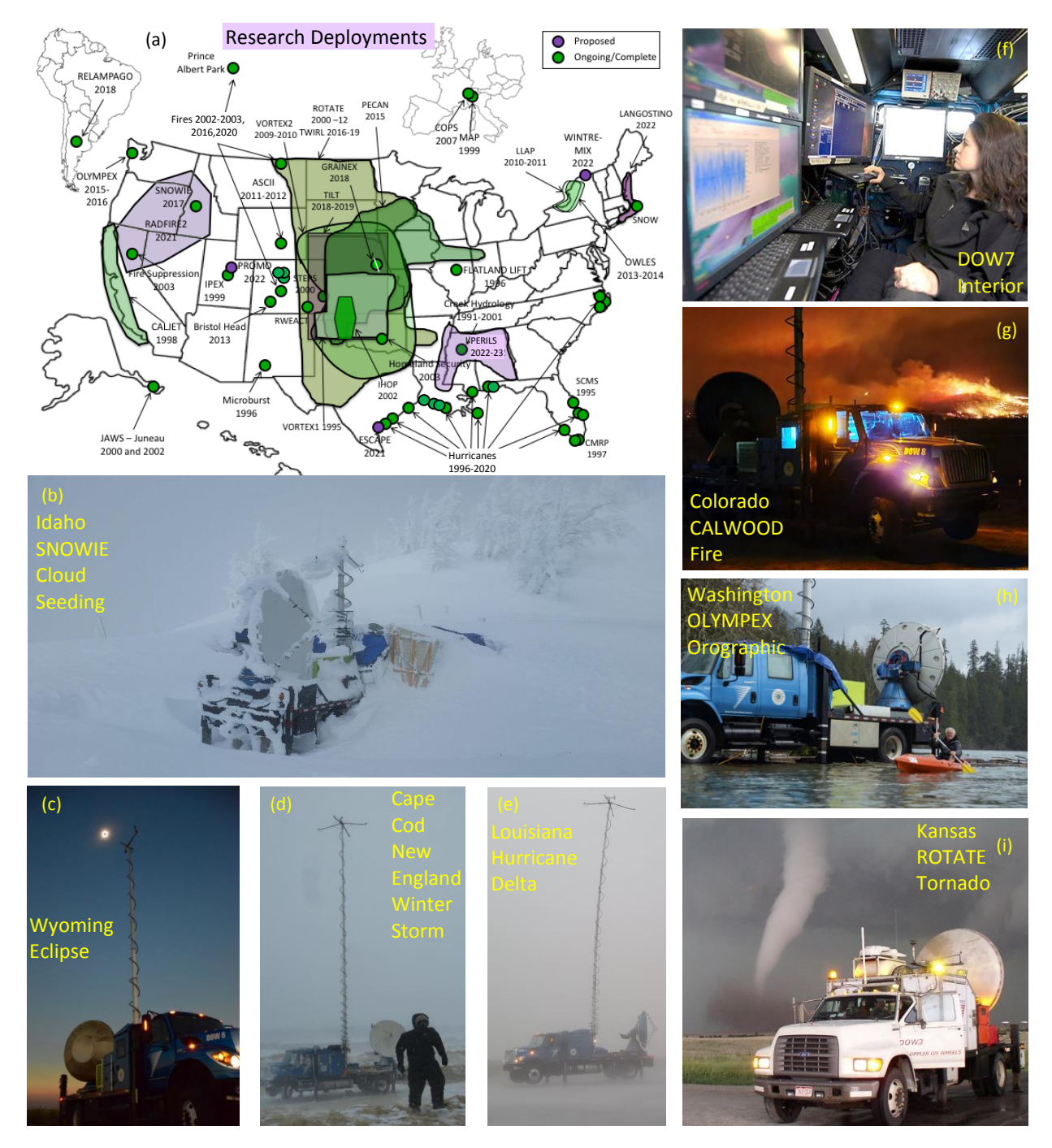


Figure 3. Sample DOW deployments. (a) schematic map of study domains, (b) DOW largely buried in snow at Snowbank, Idaho (2017), (c) DOW observing boundary layer during eclipse (2017), (d) DOW on Cape Cod during Nor'easter (2015), (e) DOW during hurricane Delta (2020) (f) DOW7 cabin interior, (g) DOW observing CalWood fire (2020), (h) Flooded DOW site in Lake Quinault during OLYMPEX (2016), (i) DOW scanning a tornado (2005).

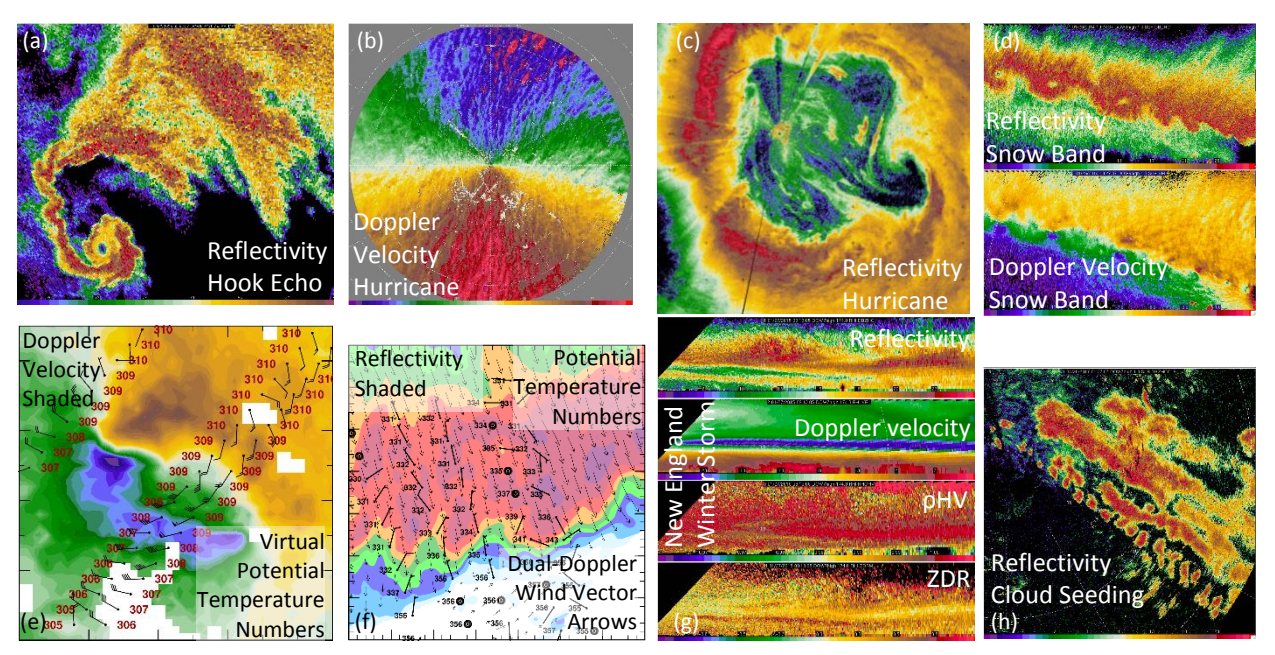


Figure 4. Illustrative FARM data images. (a) Tornadic hook echo, (b) hurricane boundary layer rolls, (c) interior view of hurricane eye with mesovortices, (d) lake-effect snow band misovortices, (e) integrated radar and in-situ observations of a tornado, (f) integrated radar and in-situ observations in a mesoscale convective system, (g) vertical (RHI) slice of microphysical layering during nor'easter, (h) snow bands/cells caused by cloud seeding.

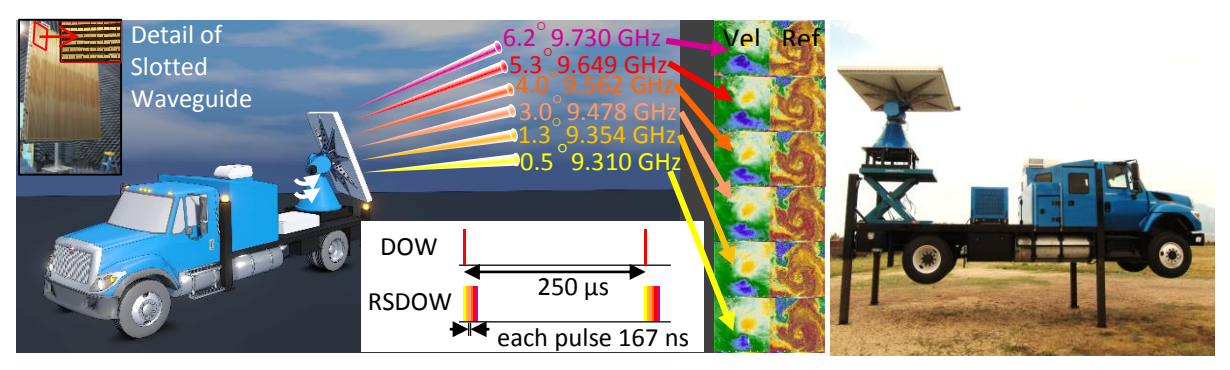


Figure 5. (left) Rapid-Scan DOW (RSDOW) slotted waveguide antenna transmits several simultaneous beams at different elevations using stepped-chirp pulses. Simplified DOW and RSDOW pulse sequences are compared schematically. Mechanical azimuthal scanning rakes the sky at all the elevations, resulting in volumetric data every 7 s. (center) Simultaneous Doppler velocity and Reflectivity slices from different elevations in a tornado. (right) RSDOW with legs and scissor lift extended.

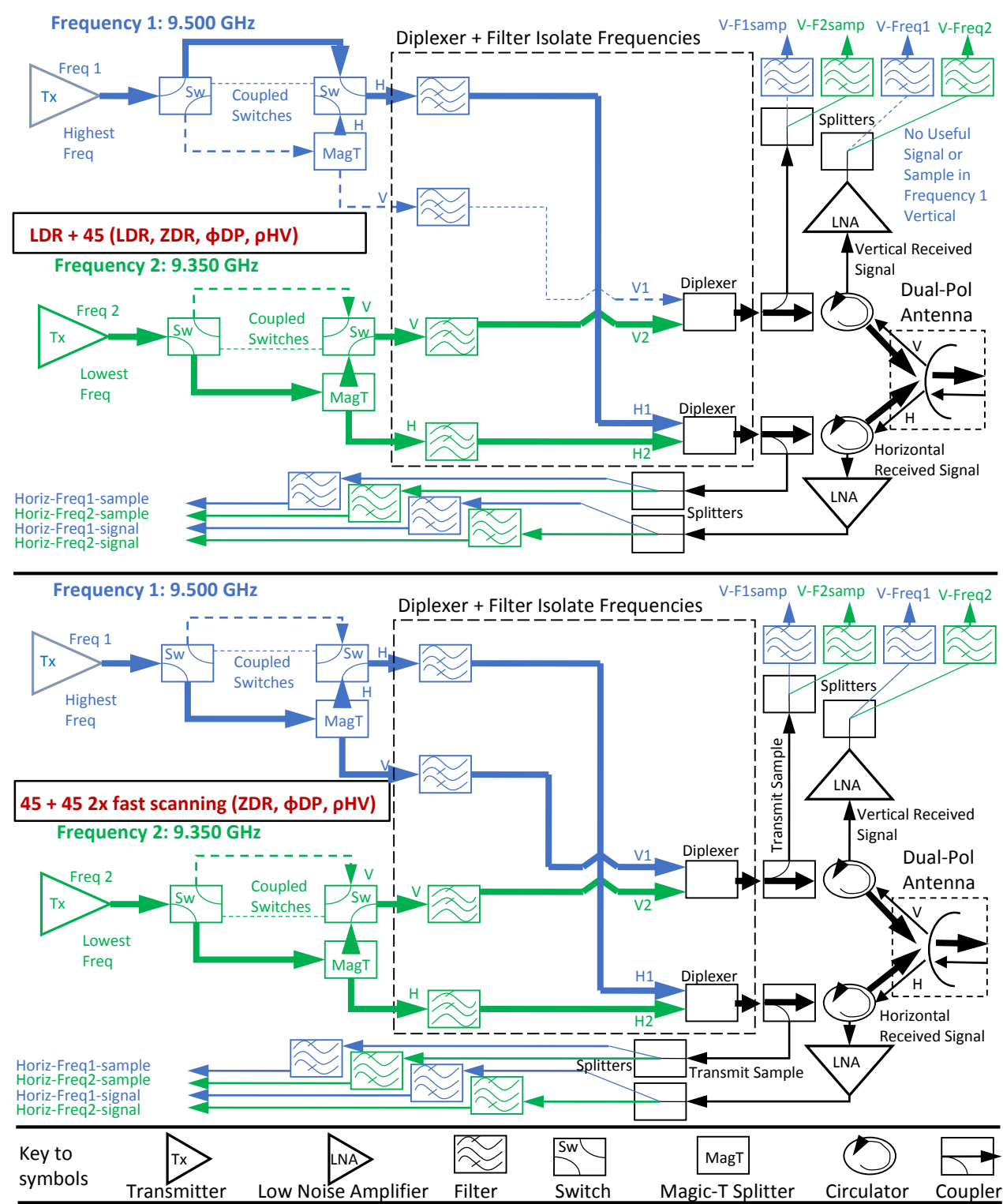


Figure 6. Simplified block diagram of Dual-Frequency Dual-Polarization (DPDF) DOW design. (top) In LDR+45 mode, Frequency 1 (blue paths) is transmitted at horizontal polarization and frequency 2 (green paths) at 45°, permitting LDR calculation. Both frequencies are combined in diplexers, then transmitted and received quasi-simultaneously (black paths) (bottom) Flipping coupled switches enables Fast-45 mode, in which both frequencies are transmitted at 45°, resulting in doubled independent samples, permitting twice-as-fast dual-polarization scanning. Heavy lines indicate "hot" transmission paths. Horizontal and vertical polarization received signals and transmit pulse samples are sent to receivers and signal processors.

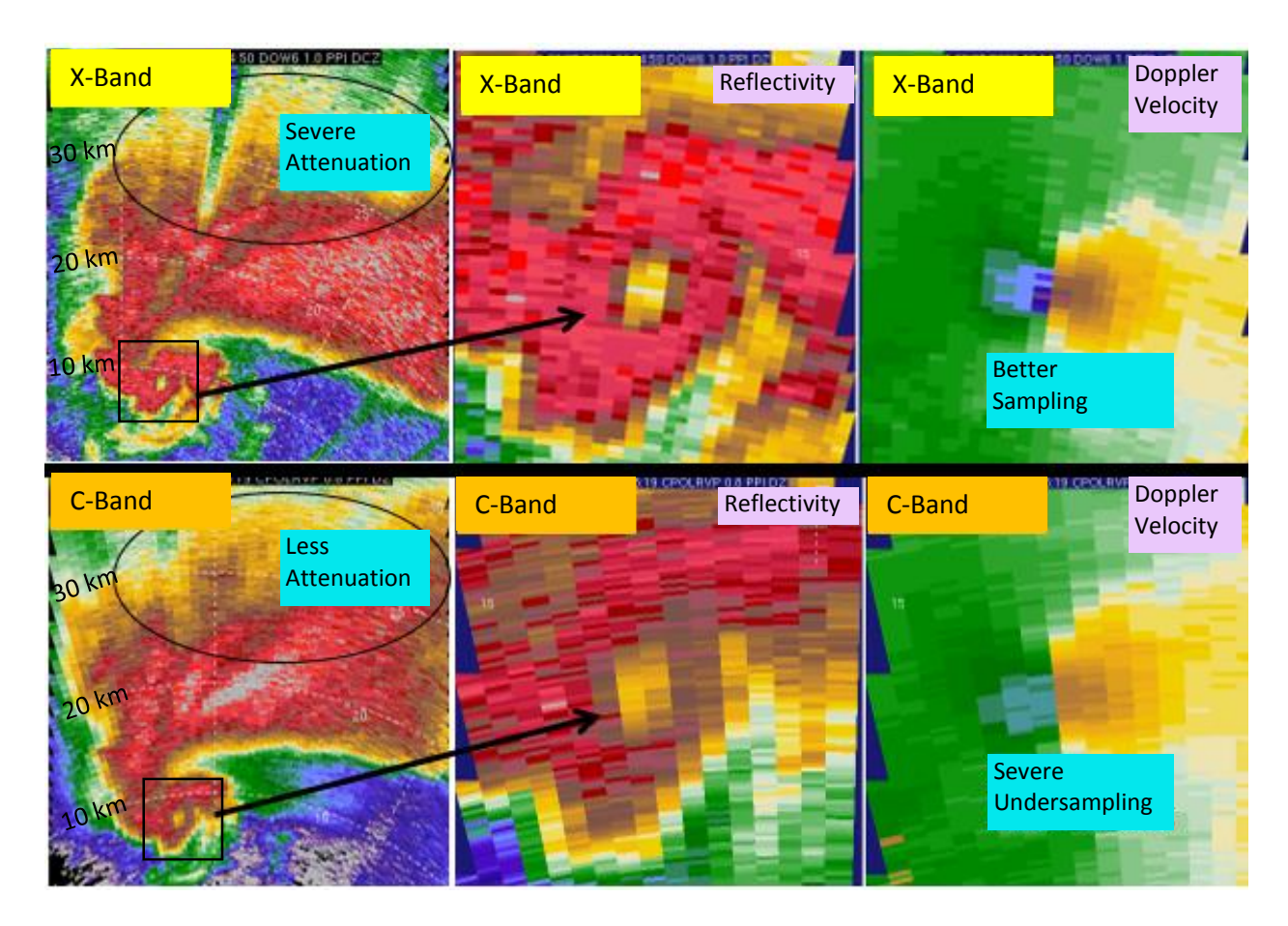


Figure 7. C-band vs X-band attenuation and resolution, existing MQD radars. Comparison of SR C-band (1.6° beamwidth) and DOW X-band (0.93° beamwidth) observations of a supercell and tornado and tornado at about 10 km range to each radar, showing compromises between severe attenuation at X-band and coarse resolution at C-band. Tornado is slightly closer to C-band radar. Scans are at approximately 1° elevation.



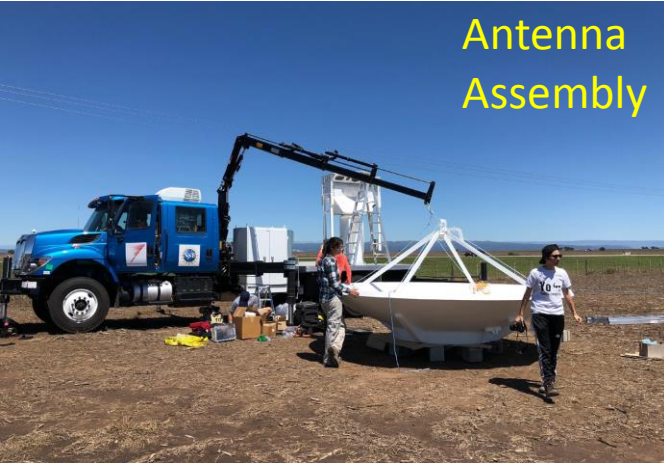






Figure 8. COW assembly. COW as transported, antenna being assembled, antenna lifted onto pedestal, deployed.



Figure 9. FARM Mobile Mesonets (MM).



Figure 10. FARM PODNET units.



Figure 11. FARM POLENET unit being deployed on power pole during hurricane Delta (2020).



Figure 12. FARM MQD sounding being launched from an MM which also carries PODNET units.



Figure 13. FARM Mobile Operations and Repair Center (MORC).

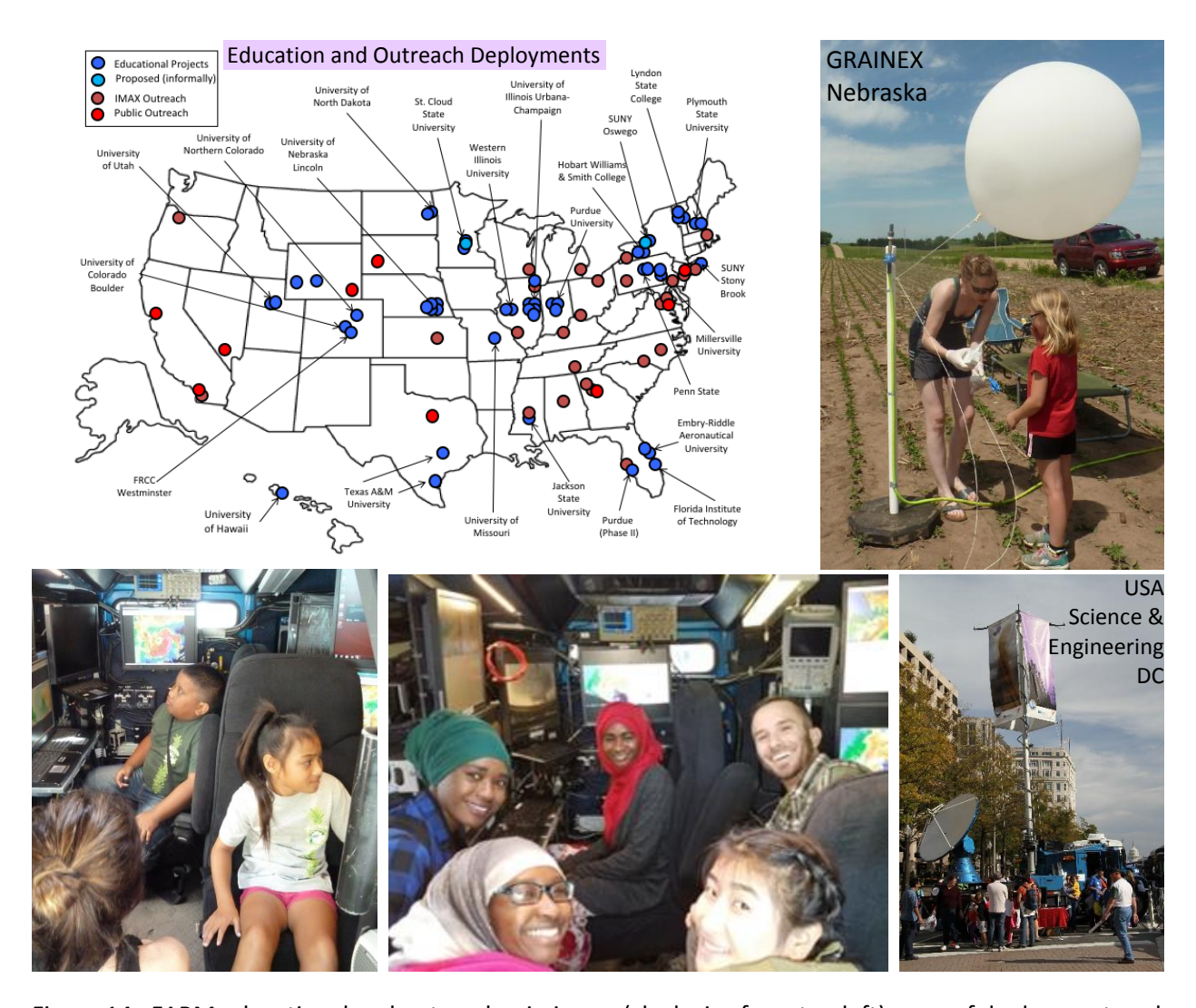


Figure 14. FARM educational and outreach missions. (clockwise from top left) map of deployments, ad hoc outreach entraining local children to launch upper air soundings during the GRAINEX field project, DOW at USA Science and Engineering Festival in Washington DC, university educational deployment, outreach with K-12 children.

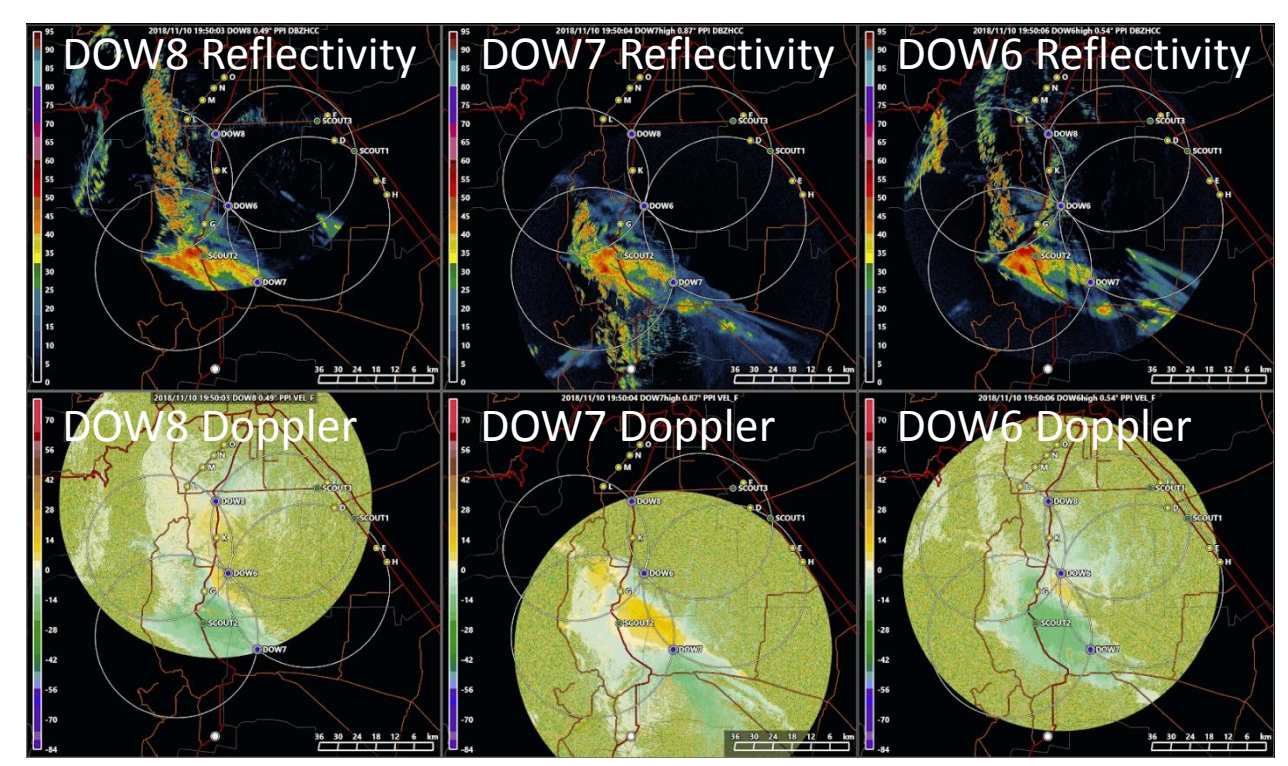


Figure 15. GURU Field Data and Coordination Display. Near real-time imagery from DOWs/COW is integrated with MM, PODNET, and sounding tracking to aid in mission planning, radar status, and field coordination. This image is from the real-time GURU display in the RELAMPAGO operations center. POD and MM locations are shown relative to DOW reflectivity and Doppler velocity fields.

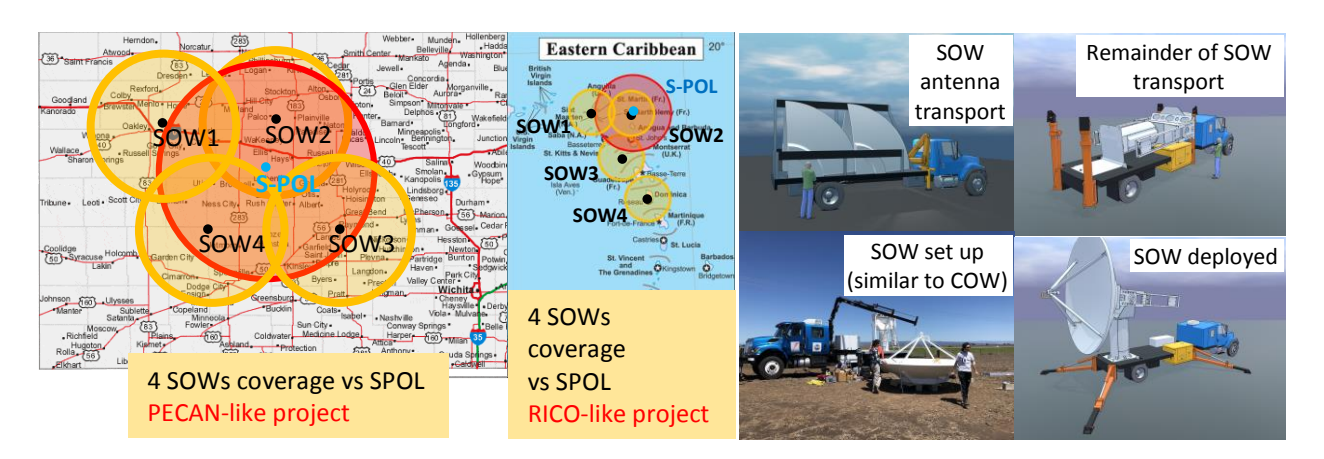


Figure 16. Comparison of SOWNET and SPOL radar coverage in hypothetical (left) PECAN- and (center) RICO-type studies. Red and orange circles enclose regions with < 1.7 km beam width (100 km range from S-POL, 67 km range from any of the SOWs). SOWNET provides greater surveillance area. Much of the yellow-shaded areas are within SOWNET multiple-Doppler vector wind coverage. (right) SOW set up is similar to COW's, requires ~6 hours, and much quicker and less expensive than larger S-band radars.

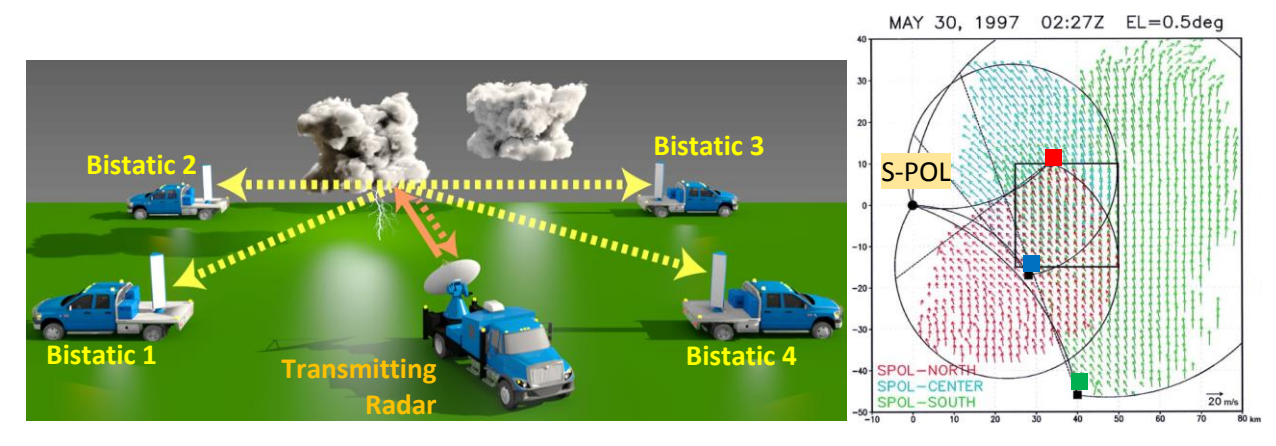


Figure 17. (left) Schematic mobile bistatic network with four receiving antennas and one transmitting radar. The transmitting radar is, in this example, a DOW or SOW, but can be a stationary radar (e.g., S-POL). The four receiving antennas are on the back of pickup trucks, but can be deployed similarly to Pods. The transmitting and receiving radars can be moved like MMs to optimize coverage and vector wind retrievals as phenomena move/evolve. As the DOW/SOW transmits and scans, the pulses in its narrow radar beam (orange arrow) are scattered from hydrometeors, dust, etc. Some of that scattered energy (dashed yellow arrows) is received by the passive antennas, as well as the by the DOW/SOW antenna (dashed orange arrow). Three-dimensional vector wind fields are calculated from these various Doppler measurements. (right) An example of vector wind retrievals from a bistatic network. In this example, there was one transmitting radar (S-POL) and three bistatic receivers (solid squares). The colored vectors depict the retrievals using data from the north (red), central (blue), and southern (green) bistatic receivers. Arcs depict the bistatic dual-Doppler lobes with the transmitting radar. The square outline encloses an overdetermined analysis domain. (Image adapted from Satoh and Wurman 2003).